

# Perfect Reconstruction Two-Channel Wavelet Filter-Banks for Graph Structured Data

Sunil K. Narang\*, *Student Member, IEEE*, and Antonio Ortega, *Fellow, IEEE*

## Abstract

In this work we propose the construction of two-channel wavelet filterbanks for analyzing functions defined on the vertices of any arbitrary finite weighted undirected graph. These graph based functions are referred to as *graph-signals* as we build a framework in which many concepts from the classical signal processing domain, such as Fourier decomposition, signal filtering and downsampling can be extended to graph domain. Especially, we observe a *spectral folding* phenomenon in *bipartite graphs* which occurs during downsampling of these graphs and produces *aliasing* in graph signals. This property of bipartite graphs, allows us to design critically sampled two-channel filterbanks, and we propose quadrature mirror filters (referred to as graph-QMF) for bipartite graph which cancel aliasing and lead to perfect reconstruction. For arbitrary graphs we present a bipartite subgraph decomposition which produces an edge-disjoint collection of bipartite subgraphs. Graph-QMFs are then constructed on each bipartite subgraph leading to “multi-dimensional” separable wavelet filterbanks on graphs. Our proposed filterbanks are critically sampled and we state necessary and sufficient conditions for orthogonality, aliasing cancellation and perfect reconstruction. The filterbanks are realized by Chebychev polynomial approximations.

**Note:** Code examples from this paper are available at [http://biron.usc.edu/wiki/index.php/Graph\\_Filterbanks](http://biron.usc.edu/wiki/index.php/Graph_Filterbanks)

**EDICS Category: DSP-WAVL, DSP-BANK, DSP-MULT, DSP-APPL, MLT**

Sunil K. Narang is with the Signal & Image Processing Institute, Ming Hsieh Department of Electrical Engineering, University of Southern California, Los Angeles, California, USA 90089 email: [narang.sunil@gmail.com](mailto:narang.sunil@gmail.com).

Antonio Ortega is with the Signal & Image Processing Institute, Ming Hsieh Department of Electrical Engineering, University of Southern California, Los Angeles, California, USA 90089 email: [antonio.ortega@sipi.usc.edu](mailto:antonio.ortega@sipi.usc.edu).

This work was supported in part by NSF under grant CCF-1018977.

## I. INTRODUCTION

### A. Motivation

Graphs provide a very flexible model for representing data in many domains. Many networks such as biological networks [1], social networks [2], [3] and sensor networks [4], [5] etc. have a natural interpretation in terms of finite graphs with vertices as data-sources and links established based on connectivity, similarity, ties etc. The data on these graphs can be visualized as a finite collection of samples termed as *graph-signals*. For example, graphical models can be used to represent irregularly sampled datasets in Euclidean spaces such as regular grids with missing samples. In many machine learning applications multi-dimensional datasets can be represented as *point-clouds* of vectors and links are established between data sources based on the distance between their feature-vectors. In computer vision, meshes are polygon graphs in 2D/3D space and the attributes of the sampled points (coordinates, intensity etc) constitute the graph-signals. The graph-signal formulation can also be used to solve systems of partial differential equations using finite element analysis (grid based solution). The sizes (number of nodes) of the graphs in these applications can be very large, which present computational and technical challenges for the purpose of storage, analysis etc. In some other applications such as wireless sensor-networks, the data-exchanges between far-off nodes can be expensive (bandwidth, latency, energy constraints issues). Therefore, instead of operating on the original graph, it would be desirable to find and operate on smaller graphs with fewer nodes and data representing a smooth<sup>1</sup> approximation of the original data. Moreover, such systems need to employ localized operations which could be computed at each node by using data from a small neighborhood of nodes around it. Multi-channel wavelet filterbanks, widely used as a signal processing tool for the sparse representation of signals, possess both these features (i.e. smooth approximations and localized operations). For example, a two channel wavelet transform splits the sample space into an approximation subspace which contains a smoother (coarser) version of the original signal and a detail subspace containing additional details required to perfectly reconstruct the original signal. A discussion of the construction and analysis of wavelet filterbanks for regular signals can be found in standard textbooks such as [6]. While wavelet transform-based techniques would seem well suited to provide efficient local analysis, a major obstacle to their application to graphs is that these, unlike images, are not regularly structured. For graphs traditional notions of dimensions along which to filter the data do not hold.

<sup>1</sup>more generally, it could be any sparse approximation of the original data.

Researchers have recently focused on developing localized transforms specifically for data defined on graphs. Crovella and Kolaczyk [2] designed wavelet like functions on graphs which are localized in space and time. These graph functions  $\psi_{j,k}$  are composed of either shifts or dilations of a single generating function  $\psi$ . Wang and Ramchandran [5] proposed graph dependent basis functions for sensor network graphs, which implement an invertible 2-channel like filter-bank. There exists a natural spectral interpretation of graph-signals in terms of eigen-functions and eigen-values of graph Laplacian matrix  $\mathbf{L}$ . Maggioni and Coifman [7] introduced “diffusion wavelets” as the localized basis functions of the eigenspaces of the dyadic powers of a diffusion operator. Hammond et. al. [8] construct a class of wavelet operators in the *graph spectral domain*, i.e., the space of eigenfunctions of the graph Laplacian matrix  $\mathbf{L}$ . These eigenfunctions provide a spectral decomposition for data on a graph similar to the Fourier transform for standard signals. A common drawback of all of these filterbank designs is that they are not critically sampled : the output of the transform is not downsampled and there is oversampling by a factor equal to the number of channels in the filterbank. Unlike classical wavelet transforms which have well-understood downsampling/upsampling operations, there is no obvious way in graphs to downsample nodes in a regular manner, since the neighboring nodes vary in number. Lifting based wavelet transforms have been proposed in [9], [10] for graphs in Euclidean Space and in our previous work for trees in [4], [11] and for general graphs in [12]. These transforms are critically sampled and invertible by construction. However the design requires splitting the vertex set of the graph into two disjoint sets and the transform is computed only on the links between nodes in different sets. Thus links between nodes in same set are not utilized by the transform.

Our contribution in this paper is to introduce a theory behind sampling operations on graphs, which leads us to the design of critically-sampled wavelet-filterbanks on graphs. We describe a *downsample then upsample (DU)* operation on graphs in which a set of nodes in the graph are first downsampled (removed) and then upsampled (replaced) by inserting zeros. This work stems from our recent results in [13], where we showed that downsampling for graph-signals defined on *k-regular bipartite graphs* is governed by a Nyquist-like theorem. In this paper, we extend the results presented in [13] to all undirected bipartite graphs and show that in these graphs, the *DU* operations lead to a spectral decomposition of the graph-signal where spectral coefficients are reproduced at mirror graph-frequencies around a central frequency. This is a phenomenon we term as *spectrum folding in graphs* as it is analogous to the frequency-folding or “aliasing” effect for regular one-dimensional signals. We utilize this property to propose two-channel filterbanks on bipartite graphs which are critically sampled and provide *necessary and sufficient* conditions for aliasing cancellation, perfect-reconstruction and orthogonality in these filterbanks. As a

practical solution we propose a *graph-quadrature mirror filterbank* (referred to as graph-QMF) design for bipartite graphs which has all the above mentioned properties. However, the exact realizations of the graph-QMF filters do not have well-localized support on the graph and therefore we implement polynomial approximations of these filters which are locally supported around each node (at the cost of small reconstruction error and loss of orthogonality). For arbitrary graphs, we formulate a bipartite subgraph decomposition problem well known to the graph-theory community. The decomposition provides us an edge-disjoint collection of  $K$  bipartite subgraphs, each with the same vertex set  $\mathcal{V}$  and whose union is the original graph. Each of these subgraphs is then used as a separate “dimension” to filter and downsample leading to a  $K$ -dimensional separable wavelet filterbank design. To the best of our knowledge no such invertible and critically sampled two-channel filter-bank designs have been proposed for arbitrary graphs before. The outline for the rest of the paper is as follows: we describe the basic framework to understand graph-based transforms in Section II. In this section we also describe and evaluate some of the existing work on wavelet-like transforms on graph. In Section III we propose our solution and in Section IV we demonstrate the utility of proposed filterbanks by conducting some experiments. Finally, in Section V, we conclude and describe our future work.

## II. PRELIMINARIES

We use the common convention of representing matrices and vectors with bold letters, sets with calligraphic capital letters and scalars with normal letters. A graph can be denoted as  $G = (\mathcal{V}, E)$  with vertices (or nodes) in set  $\mathcal{V}$  and links (or edges) as tuples  $(i, j)$  in  $E$ . We only consider undirected graphs without self-loops in our work. The size of the graph  $N = |\mathcal{V}|$  is the number of nodes and geodesic distance metric is given as  $d(v, m)$ . The  $j$ -hop neighborhood  $\mathcal{N}_{j,n} = \{v \in \mathcal{V} : d(v, n) \leq j\}$  of node  $n$  is the set of all nodes which are at most  $j$ -hop distance away from node  $n$ . Algebraically, a graph can be represented with the node-node adjacency matrix  $\mathbf{A}$  such that the element  $A(i, j)$  is the weight of the edge between node  $i$  and  $j$  (0 if no edge). The value  $d_i$  is the degree of node  $i$ , which is the sum of weights of all edges connected to node  $i$ , and  $\mathbf{D} = \text{diag}(\{d_i\})$  denotes the diagonal degree matrix whose  $i^{\text{th}}$  diagonal entry is  $d_i$ . The Laplacian matrix of the graph is defined as  $\mathbf{L} = \mathbf{D} - \mathbf{A}$  and has a normalized form  $\mathcal{L} = \mathbf{I} - \mathbf{D}^{-1/2}\mathbf{A}\mathbf{D}^{-1/2}$ , where  $\mathbf{I}$  is the identity matrix. We denote  $\langle \mathbf{f}_1, \mathbf{f}_2 \rangle$  as the inner-product between vectors  $\mathbf{f}_1$  and  $\mathbf{f}_2$ .

### A. Spatial Representation of Graph Signals

A graph signal is a real-valued scalar function  $f : \mathcal{V} \rightarrow \mathbb{R}$  defined on graph  $G = (\mathcal{V}, E)$  such that  $f(v)$  is the sample value of function at vertex  $v \in \mathcal{V}$ .<sup>2</sup> On a finite graph, the graph-signal can be viewed as a sequence or a vector  $\mathbf{f} = [f(0), f(1), \dots, f(N)]^t$ , where the order of arrangement of the samples in the vector is arbitrary and neighborhood (or nearness) information is provided separately by the adjacency matrix  $\mathbf{A}$ . Graph-signals can, for example, be a set of measured values by sensor network nodes [5] or traffic measurement samples on the edges of an Internet graph [2] or information about the actors in a social network. Further, a graph based transform is defined as a linear transform  $\mathbf{T} : \mathbb{R}^N \rightarrow \mathbb{R}^M$  applied to the  $N$ -node graph-signal space, such that the operation at each node  $n$  is a linear combination of the value of the graph-signal  $f(n)$  at the node  $n$  and the values  $f(m)$  on nearby nodes  $m \in \mathcal{N}_{j,n}$ , i.e.,

$$y(n) = T(n, n)f(n) + \sum_{m \in \mathcal{N}_{j,n}} T(n, m)f(m) \quad (1)$$

In analogy to the 1-D regular case, we would sometimes refer to graph-transforms as graph-filters and the elements  $T(n, m)$  for  $m = 1, 2, \dots, N$  as the filter coefficients at the  $n^{\text{th}}$  node. A graph transform is said to be strictly  $j$ -hop localized in the spatial domain of the graph if the filter coefficients  $T(n, m)$  are zero beyond the  $j$ -hop neighborhood of each node  $n$ . Note that spatial localization can also be applied in a weaker sense in which filter coefficients  $T(n, m)$  decay sharply in magnitude beyond  $j$ -hop neighborhood of node  $n$ .

### B. Spectral Representation of Graph Signals

The Laplacians  $\mathbf{L}$  and  $\mathcal{L}$  are both symmetric positive semidefinite matrices and therefore, from the spectral projection theorem, there exists a real unitary matrix  $\mathbf{U}$  which diagonalizes  $\mathcal{L}$ , such that  $\mathbf{U}^t \mathcal{L} \mathbf{U} = \mathbf{\Lambda} = \mathbf{diag}\{\lambda_i\}$  is a non-negative diagonal matrix. This leads to an *eigenvalue decomposition* of matrix  $\mathcal{L}$  given as

$$\mathcal{L} = \mathbf{U} \mathbf{\Lambda} \mathbf{U}^t = \sum_{i=1}^N \lambda_i \mathbf{u}_i \mathbf{u}_i^t, \quad (2)$$

where the eigenvectors  $\mathbf{u}_1, \mathbf{u}_2, \dots, \mathbf{u}_N$ , which are columns of  $\mathbf{U}$  form a basis in  $\mathbb{R}^N$  and the corresponding eigenvalues  $\sigma(G) = \{0 \leq \lambda_1 \leq \lambda_2 \leq \dots \leq \lambda_N\}$  represent  $N$  orthogonal eigen-spaces  $V_{\lambda_i}$  with projection matrices  $\mathbf{u}_i \mathbf{u}_i^t$ . Thus, every graph-signal  $\mathbf{f} \in \mathbb{R}^N$  can be decomposed into a linear combination of eigenvectors  $\mathbf{u}_i$  given as  $\mathbf{f} = \sum_{n=1}^N \bar{f}(n) \mathbf{u}_n$ . It has been shown in [14], [15] that the eigenvectors of

<sup>2</sup> The extension to complex or vector sample values  $f(v)$  is possible but is not considered in this work.

Laplacian matrix provide a harmonic analysis of graph signals which gives a Fourier-like interpretation. The eigenvectors act as the *natural vibration modes* of the graph, and the corresponding eigenvalues as the associated *graph-frequencies*. The *spectrum*  $\sigma(G)$  of a graph is defined as the set of eigen-values of its normalized Laplacian matrix and it is always a subset of closed set  $[0, 2]$  for any graph  $G$ . Any eigenvector  $\mathbf{u}_\lambda$  is considered to be a low pass eigenvector if the magnitude of the corresponding eigenvalue  $\lambda$  is small, i.e., close to 0. Similarly, an eigenvector is a high-pass eigenvector if its eigenvalue is large, i.e., close to the highest graph-frequency.<sup>1</sup> The *graph Fourier transform* (GFT), denoted as  $\bar{f}$ , is defined in [8] as the projections of a signal  $\mathbf{f}$  on the graph  $G$  onto the eigenvectors of  $G$ , i.e.,

$$\bar{f}(\lambda) = \langle \mathbf{u}_\lambda, \mathbf{f} \rangle = \sum_{i=1}^N f(i)u_\lambda(i). \quad (3)$$

Note that GFT is an energy preserving transform and a signal can be considered low-pass (or high-pass) if the energy  $|\bar{f}(\lambda)|^2$  of the GFT coefficients is mostly concentrated on the low-pass (or high-pass) eigenvectors. In case of eigenvalues with multiplicity greater than 1 (say  $\lambda_1 = \lambda_2 = \lambda$ ) the eigenvectors  $\mathbf{u}_1, \mathbf{u}_2$  are unique up to a unitary transformation in the eigenspace  $V_\lambda = V_{\lambda_1} = V_{\lambda_2}$ . In this case we can choose  $\lambda_1 \mathbf{u}_1 \mathbf{u}_1^t + \lambda_2 \mathbf{u}_2 \mathbf{u}_2^t = \lambda \mathbf{P}_\lambda$  where  $\mathbf{P}_\lambda$  is the projection matrix for eigenspace  $V_\lambda$ . Note that for all symmetric matrices, the dimension of eigenspace  $V_\lambda$  (geometric multiplicity) is equal to the multiplicity of eigenvalue  $\lambda$  (algebraic multiplicity) and the spectral decomposition in (2) can be written as

$$\mathcal{L} = \sum_{\lambda \in \sigma(\mathbf{G})} \lambda \sum_{\lambda_i = \lambda} \mathbf{u}_i \mathbf{u}_i^t = \sum_{\lambda \in \sigma(\mathbf{G})} \lambda \mathbf{P}_\lambda. \quad (4)$$

The eigenspace projection matrices are idempotent and  $\mathbf{P}_\lambda$  and  $\mathbf{P}_\gamma$  are orthogonal if  $\lambda$  and  $\gamma$  are distinct eigenvalues of the Laplacian matrix, i.e.,

$$\mathbf{P}_\lambda \mathbf{P}_\gamma = \delta(\lambda - \gamma) \mathbf{P}_\lambda, \quad (5)$$

where  $\delta(\lambda)$  is the Kronecker delta function.

### C. Downsampling in Graphs

We define the downsampling operation  $\beta_H$  on the graph  $G = (\mathcal{V}, E)$  as choosing a subset  $H \subset \mathcal{V}$  such that all samples of the graph signal  $\mathbf{f}$ , corresponding to indices not in  $H$ , are discarded. A subsequent

<sup>1</sup>The mapping  $\mathbf{u}_n \rightarrow \mathcal{V}$  associates the real numbers  $u_n(i), i = \{1, 2, \dots, N\}$ , with the vertices  $\mathcal{V}$  of  $G$ . The numbers  $u_n(i)$  will be positive, negative or zero. The frequency interpretation of eigenvectors can thus be understood in terms of number of zero-crossings (pair of nodes with different signs) of eigenvector  $\mathbf{u}_n$  on the graph  $G$ . For any finite graph the eigenvectors with large eigenvalues have more zero-crossings (hence high-frequency) than eigenvectors with small eigenvalues. These results are related to ‘nodal domain theorems’ and readers are directed to [16] for more details.

upsampling operation projects the downsampled signal back to original  $\mathbb{R}^N$  space by inserting zeros in place of discarded samples in  $H^c = L$ . Given such a set  $H$  we define a *downsampling function*  $\beta_H \in \{-1, +1\}$  given as

$$\beta_H(n) = \begin{cases} 1 & \text{if } n \in H \\ -1 & \text{if } n \notin H \end{cases} \quad (6)$$

and a diagonal *downsampling matrix*  $\mathbf{J}_{\beta_H} = \text{diag}\{\beta_H(n)\}$ . The overall ‘downsample then upsample’ (*DU*) operation can then be algebraically represented as

$$f_{du}(n) = \frac{1}{2}(1 + \beta_H(n))f(n) \quad (7)$$

and in matrix form as

$$\mathbf{f}_{du} = \frac{1}{2}(\mathbf{I} + \mathbf{J}_{\beta_H})\mathbf{f} \quad (8)$$

Note that  $\mathbf{J}_{\beta_H}$  is a symmetric matrix such that  $\mathbf{J}_{\beta_H}^2 = \mathbf{I}$  (identity matrix). Since the graph-signal after *DU* operation also belongs to  $\mathbb{R}^N$ , it too has a GFT decomposition  $\bar{\mathbf{f}}_{du}$  according to (3). The relationship between the GFTs of  $\mathbf{f}$  and  $\mathbf{f}_{du}$  is given as:

$$\bar{f}_{du}(l) = \langle \mathbf{u}_l, \mathbf{f}_{du} \rangle = \frac{1}{2}(\langle \mathbf{u}_l, \mathbf{f} \rangle + \langle \mathbf{u}_l, \mathbf{J}_{\beta_H} \mathbf{f} \rangle) \quad (9)$$

The inner-product  $\langle \mathbf{u}_l, \mathbf{J}_{\beta_H} \mathbf{f} \rangle$  can also be written as  $\langle \mathbf{J}_{\beta_H} \mathbf{u}_l, \mathbf{f} \rangle$ , which represents the projection of input signal  $\mathbf{f}$  onto a *deformed* eigenvector  $\mathbf{J}_{\beta_H} \mathbf{u}_l$ . We define this projection as a *deformed* spectral coefficient  $\bar{f}^d(l)$  and (9) can be written as:

$$\bar{f}_{du}(l) = \frac{1}{2}(\bar{f}(l) + \langle \mathbf{J}_{\beta_H} \mathbf{u}_l, \mathbf{f} \rangle) = \frac{1}{2}(\bar{f}(l) + \bar{f}^d(l)) \quad (10)$$

In case of bipartite graphs, the spectrum of the graph is symmetric and the deformed eigenvectors are also the eigenvectors of the same graph. This phenomenon, termed as *spectral folding*, forms the basis of our two-channel filterbank framework, and will be described in detail in Section III.

#### D. Two-Channel Filterbanks on Graph

A two-channel wavelet filterbank on a graph provides a decomposition of any graph-signal into a lowpass (smooth) graph-signal and a highpass (detail) graph-signal component. The two channels of the filterbanks are characterized by the graph-filters  $\{\mathbf{H}_i, \mathbf{G}_i\}_{i \in \{0,1\}}$  and the downsampling operations  $\beta_H$  and  $\beta_L$  as shown in Figure 1. The transform  $\mathbf{H}_0$  acts as a lowpass filter, i.e., it transfers the

contributions of the low-pass graph-frequencies which are below some cut-off and attenuates significantly the graph-frequencies which are above the cut-off. The highpass transform  $\mathbf{H}_1$  does the opposite of a low-pass transform, i.e, it attenuates significantly, the graph-frequencies below some cut-off frequency. The filtering operations in each channel are followed by downsampling operations  $\beta_H$  and  $\beta_L$ , which means that the nodes with membership in the set  $H$  store the output of highpass channel while the nodes in the set  $L$  store the output of lowpass channel. For critically sampled output we have:  $|H| + |L| = N^2$ . Using (8), it is easy to see from Figure 1 that the output signals in the lowpass and highpass channels,

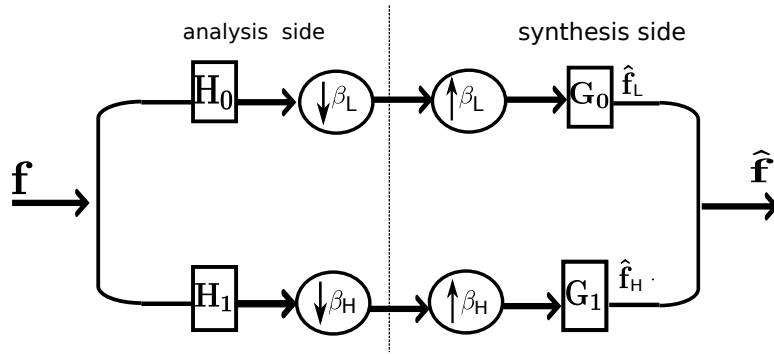


Fig. 1: Block diagram of a two-channel wavelet filterbank on graph.

after reconstruction are given as

$$\begin{aligned}\hat{\mathbf{f}}_L &= \frac{1}{2}\mathbf{G}_0(\mathbf{I} + \mathbf{J}_{\beta_L})\mathbf{H}_0\mathbf{f} \\ \hat{\mathbf{f}}_H &= \frac{1}{2}\mathbf{G}_1(\mathbf{I} + \mathbf{J}_{\beta_H})\mathbf{H}_1\mathbf{f},\end{aligned}\quad (11)$$

respectively. The overall output  $\hat{\mathbf{f}}$  of the filterbank is the sum of outputs of the two channels, i.e.,  $\hat{\mathbf{f}} = \hat{\mathbf{f}}_L + \hat{\mathbf{f}}_H = \mathbf{T}\mathbf{f}$ , where  $\mathbf{T}$  is the overall transfer function of the filterbank given as:

$$\begin{aligned}\mathbf{T} &= \frac{1}{2}\mathbf{G}_0(\mathbf{I} + \mathbf{J}_{\beta_L})\mathbf{H}_0 + \frac{1}{2}\mathbf{G}_1(\mathbf{I} + \mathbf{J}_{\beta_H})\mathbf{H}_1 \\ &= \underbrace{\frac{1}{2}(\mathbf{G}_0\mathbf{H}_0 + \mathbf{G}_1\mathbf{H}_1)}_{\mathbf{T}_{eq}} + \underbrace{\frac{1}{2}(\mathbf{G}_0\mathbf{J}_{\beta_L}\mathbf{H}_0 + \mathbf{G}_1\mathbf{J}_{\beta_H}\mathbf{H}_1)}_{\mathbf{T}_{alias}},\end{aligned}\quad (12)$$

where  $\mathbf{T}_{eq}$  is the transfer function of the filterbank without the  $DU$  operation and  $\mathbf{T}_{alias}$  is another transform which arises primarily due to the downsampling in the two channels. For perfect reconstruction

<sup>2</sup> Note that in the regular signal domain the two most common patterns of critically sampled output are i)  $H = L = \{0, 2, 4, \dots\}$ , where even set of nodes store the output of both channels and ii)  $L = \{0, 2, 4, \dots\}$  and  $H = \{1, 3, 5, \dots\}$ , where each node stores the output of only one of the channel.



$\mathbf{T}$  should be equal to identity which can be ensured by requiring  $\mathbf{T}_{eq}$  to be a scalar multiple of identity and  $\mathbf{T}_{alias} = \mathbf{0}$ . Thus the two-channel filterbank on a graph provides distortion-free perfect reconstruction if

$$\begin{aligned}\mathbf{G}_0 \mathbf{J}_{\beta_L} \mathbf{H}_0 + \mathbf{G}_1 \mathbf{J}_{\beta_H} \mathbf{H}_1 &= \mathbf{0} \\ \mathbf{G}_0 \mathbf{H}_0 + \mathbf{G}_1 \mathbf{H}_1 &= c \mathbf{I}\end{aligned}\quad (13)$$

In order to design perfect reconstruction filterbanks we need to determine a) how to design filtering operations  $\mathbf{H}_i, \mathbf{G}_i, i = \{0, 1\}$ , and b) the downsampling functions  $\beta_L$  and  $\beta_H$ . In Section III, we show that the spectral folding phenomenon in bipartite graphs leads to an aliasing interpretation of (13) and we design filterbanks which cancel aliasing and lead to perfect reconstruction of any graph-signal. Before explaining our approach, we briefly analyze and evaluate some of the existing graph based transforms, by representing them using the framework we just introduced.

### E. Existing Designs

Existing designs of wavelet-like filterbanks on the graph can be divided into two types, namely, spatial and spectral designs. In order to understand these designs we introduce some additional notation. We define  $\partial\mathcal{N}_{h,k}$  to be an  $h$ -hop neighborhood ring around node  $k$  (i.e., the set of all nodes which are exactly  $h$  hops away from node  $k$ ), a  $j$ -hop adjacency matrix  $\mathbf{A}_j$  s.t.  $\mathbf{A}_j(n, m) = 1$  only if  $m \in \mathcal{N}_{j,n}$ , a  $j$ -hop diagonal degree matrix with  $D_j(k, k) = |\mathcal{N}_{j,k}|$  s.t.  $d_{j,k} = |\mathcal{N}_{j,k}|$  and a  $j$ -hop uniform Laplacian matrix  $\mathbf{L}_j = \mathbf{D}_j - \mathbf{A}_j$ . Similarly we define a ring adjacency matrix  $\partial\mathbf{A}_h$  such that  $\partial\mathbf{A}_h(n, m) = 1$  only if  $m \in \partial\mathcal{N}_{h,n}$  and corresponding ring degree matrix  $\partial\mathbf{D}_h = \text{diag}\{\partial d_{j,k}\}$  s.t.  $\partial d_{j,k} = |\partial\mathcal{N}_{h,k}|$ .

1) *Spatial Designs*: Wang and Ramchandran [5] proposed spatially localized graph transforms for sensor network graphs with binary links, (i.e. links which have weight either 0 or 1). The transforms proposed in [5] either compute a weighted average given as

$$y(n) = \left(1 - a + \frac{a}{d_{j,k} + 1}\right)x(n) + \sum_{m \in \mathcal{N}_{j,n}} \frac{a}{d_{j,k} + 1} x(m), \quad (14)$$

or a weighted difference given as

$$y(n) = \left(1 + b - \frac{b}{d_{j,k} + 1}\right)x(n) - \sum_{m \in \mathcal{N}_{j,n}} \frac{b}{d_{j,k} + 1} x(m), \quad (15)$$

in a  $j$ -hop neighborhood around each node in the graph. The corresponding transform matrices can be represented for a given  $j$  as

$$\begin{aligned}\mathbf{T}_j &= \mathbf{I} - a(\mathbf{I} + \mathbf{D}_j)^{-1}\mathbf{L}_j \\ \mathbf{S}_j &= \mathbf{I} + b(\mathbf{I} + \mathbf{D}_j)^{-1}\mathbf{L}_j.\end{aligned}\tag{16}$$

This approach intuitively defines a two-channel wavelet filter-bank on the graph consisting of two types of linear filters: a) *approximation filters* as given in (14) and b) *detail filters* as given in (15). However, these transforms are oversampled and produce output of the size twice that of the input. Further none of the transforms can be called a wavelet filter since both transforms have a non-zero DC response.

Crovella and Kolaczyk [2] designed wavelet like transforms on graphs which are localized in space. They defined a collection of functions  $\psi_{j,n} : \mathcal{V} \rightarrow \mathbb{R}$ , localized with respect to a range of scale/location indices  $(j, n)$ , which at a minimum satisfy  $\sum_{m \in \mathcal{V}} \psi_{j,n}(m) = 0$  (i.e. a zero DC response). Each function  $\psi_{j,n}$  is constant within hop rings  $\partial\mathcal{N}_{h,n}$  and can be written as:

$$y(n) = a_{j,0}x(n) + \sum_{h=1}^j \sum_{m \in \mathcal{N}_{h,n}} \frac{a_{j,h}}{\partial d_{j,n}} x(m)\tag{17}$$

In matrix form the  $j$ -hop wavelet transform  $\mathbf{T}_j$  can be written as:

$$\mathbf{T}_j = a_{j,0}\mathbf{I} + a_{j,1}\partial\mathbf{D}_1^{-1}\partial\mathbf{A}_1 + \dots a_{j,j}\partial\mathbf{D}_j^{-1}\partial\mathbf{A}_j\tag{18}$$

Further, the constants  $a_{j,h}$  satisfy  $\sum_{h=0}^j a_{j,h} = 0$ , which allows the wavelet filters to have zero DC response. . Though these transforms are local and provide a multi-scale summarized view of the graph, they do not have approximation filters and are not invertible in general.

Lifting based wavelet transforms for graphs have been proposed in [9], [4], [12], [10] and provide a natural way of constructing local two-channel critically sampled filter-banks on graph-signals. In this approach the vertex set is first partitioned into sets of even and odd nodes  $\mathcal{V} = \mathcal{O} \cup \mathcal{E}$ . The odd nodes compute their *prediction* coefficients using their own data and data from their even neighbors followed by even nodes computing their *update* coefficients using their own data and prediction coefficient of their neighboring odd nodes. The equivalent transform in matrix-form can be written as:

$$\mathbf{T}^{lift} = \begin{array}{c} \overbrace{\left[ \begin{array}{cc} \mathbf{I}_{\mathcal{O}} & 0 \\ \mathbf{U} & \mathbf{D}_{\mathcal{E}} \end{array} \right]}^{\text{update}} \overbrace{\left[ \begin{array}{cc} \mathbf{D}_{\mathcal{O}} & -\mathbf{P} \\ 0 & \mathbf{I}_{\mathcal{E}} \end{array} \right]}^{\text{predict}} \end{array}\tag{19}$$

where  $\mathbf{D}_{\mathcal{O}}$  and  $\mathbf{D}_{\mathcal{E}}$  are diagonal matrices of size  $|\mathcal{O}|$  and  $|\mathcal{E}|$  respectively. Although the lifting scheme

can be applied to any arbitrary graph, the design is equivalent to simplification of the graph to a bipartite (2-colorable) graph, given that nodes of the same color/parity cannot use each other's data even if they are connected by an edge. This results in edge losses.

2) *Spectral Designs*: Maggioni and Coifman [7] introduced "diffusion wavelets", a general theory for wavelet decompositions based on compressed representations of powers of a diffusion operator (such as Laplacian). Their construction interacts with the underlying graph or manifold space through repeated applications of a diffusion operator  $\mathbf{T}$ , such as the graph Laplacian  $\mathbf{L}$ . The localized basis functions at each resolution level are orthogonalized and downsampled appropriately to transform sets of orthonormal basis functions through a variation of the Gram-Schmidt orthonormalization (GSM) scheme. Although this local GSM method orthogonalizes the basis functions (filters) into well localized 'bump-functions' in the spatial domain, it does not provide guarantees on the size of the support of the filters it constructs. Further the diffusion wavelets form an over-complete basis and there is no simple way of representing the corresponding transform  $\mathbf{T}$ .

Hammond et al [8] defined spectral graph wavelet transforms that are determined by the choice of a kernel function  $g : \mathbb{R}^+ \rightarrow \mathbb{R}^+$ . The kernel  $g(\lambda)$  is a continuous bandpass function in spectral domain with  $g(0) = 0$  and  $\lim_{\lambda \rightarrow \infty} g(\lambda) = 0$ . The corresponding wavelet operator  $\mathbf{T}_g = g(\mathcal{L}) = \mathbf{U}g(\mathbf{\Lambda})\mathbf{U}^t$  acts on a graph signal  $\mathbf{f}$  by modulating each Fourier mode as

$$\mathbf{T}_g \mathbf{f} = \sum_{k=1}^N g(\lambda_k) \bar{f}(k) \mathbf{u}_k \quad (20)$$

The kernel can be scaled as  $g(t\lambda)$  by a continuous scalar  $t$ . For spatial localization, the authors design filters by approximating the kernels  $g(\lambda)$  with smooth polynomial functions. The approximate transform with polynomial kernel of degree  $k$  is given by  $\mathbf{T}_{\hat{g}} = \hat{g}(\mathcal{L}) = \sum_{l=0}^k a_l \mathcal{L}^l$  and is exactly  $k$ -hop localized in space. By construction the spectral wavelet transforms have zero DC response, hence in order to stably represent the low frequency content of signal  $\mathbf{f}$  a second class of kernel function  $h : \mathbb{R}^+ \rightarrow \mathbb{R}^+$  is introduced which acts as a lowpass filter, and satisfies  $h(0) > 0$  and  $\lim_{\lambda \rightarrow \infty} h(\lambda) = 0$ . Thus a multi-channel wavelet transform can be constructed from the choice of a low pass kernel  $h(\lambda)$  and  $J$  band-pass kernels  $\{g(t_1\lambda), \dots, g(t_J\lambda)\}$  and it is been shown that the perfect reconstruction of the original signal is assured if the quantity  $G(\lambda) = h(\lambda)^2 + \sum_{k=1}^J g(t_k\lambda)^2 > 0$  on the spectrum of  $\mathcal{L}$  (i.e., at the  $N$  eigenvalues of  $\mathcal{L}$ ). However, these transforms are overcomplete, for example, a  $J$ -scale decomposition of graph-signal of size  $N$  produces  $(J + 1)N$  transform coefficients. As a result, the transform is invertible only by the least square projection of the output signal onto a lower dimension subspace.

To conclude this section, Table I presents a summary of existing methods and their properties.<sup>3</sup>

Method	DC response	Critical Sampling	Perfect Re-construction	Orthogonality	Requires Graph Simplification
Wang & Ramchandran [5]	non-zero	No	Yes	No	No
Crovella & Kolaczyk [2]	zero	No	No	No	No
Lifting Scheme [12]	zero for wavelet basis	Yes	Yes	No	Yes
Diffusion Wavelets [7]	zero for wavelet basis	No	Yes	Yes	No
Spectral Wavelets [8]	zero for wavelet basis	No	Yes	No	No
Proposed graph-QMF filterbanks	zero (when degree-normalized) for wavelet basis	Yes	Yes	Yes	No

TABLE I: Evaluation of existing graph wavelet transforms.

### III. PROPOSED SOLUTION

Our proposed two-channel critically sampled graph wavelet filterbanks are shown in Figure 1. For  $DU$  operations we choose a specific downsampling pattern in which sets  $H$  and  $L$  provide a bipartition of the graph nodes i.e.,  $H \cap L = \phi$  and  $H \cup L = \mathcal{V}$ ). This implies that downsampling functions  $\beta_L(n) = -\beta_H(n) = \beta(n)$  and the nodes in  $L$  store the output of the lowpass channel whereas the nodes in the complement set  $H$  store the output of the highpass channel. The overall output after filtering and downsampling operations in both channels is critically sampled. For designing wavelet filters on graphs we exploit similar concepts of spectral decomposition as in [8]. Because of this, it is useful to define analysis wavelet filters  $\mathbf{H}_0$  and  $\mathbf{H}_1$  in terms of spectral kernels  $h_0(\lambda)$  and  $h_1(\lambda)$  respectively. Thus given the eigen-space decomposition of Laplacian matrix  $\mathcal{L}$  as in (4), the analysis filters can be represented as

$$\begin{aligned} \mathbf{H}_0 &= h_0(\mathcal{L}) = \sum_{\lambda \in \sigma(G)} h_0(\lambda) \mathbf{P}_\lambda \\ \mathbf{H}_1 &= h_1(\mathcal{L}) = \sum_{\lambda \in \sigma(G)} h_1(\lambda) \mathbf{P}_\lambda \end{aligned} \quad (21)$$

<sup>3</sup>Our proposed solutions can be perfect reconstruction and orthogonal without being local or can be local with approximate reconstruction.

Since the Laplacian matrix  $\mathcal{L}$  is real and symmetric, the filters designed in (21) are also real and symmetric. As described in Section II-D, the spectral decomposition of the output of a  $DU$  operation with downsampling function  $\beta$  yields a set of original signal coefficients and a set of deformed signal coefficients which are generated by the projection of the original signal onto deformed eigenvectors. In what follows, we take the special case of *bipartite graphs* for which the  $DU$  operation on any eigenvector produces an alias eigenvector at a mirror eigenvalue, a phenomenon, which is analogous to the “aliasing” effect observed in  $DU$  operations in regular signal domain. This property of bipartite graphs, allows us to express the perfect reconstruction conditions for the two channel graph-filterbanks, as given in (13), in simple terms. Subsequently, we state necessary and sufficient conditions for a two-channel graph filter-bank, designed using spectral transforms, to provide aliasing-cancellation, perfect reconstruction and an orthogonal decomposition of any graph-signal and propose a solution similar to quadrature mirror filters (QMF) in regular signal domain which satisfies all of the above conditions. For arbitrary graphs, we formulate a bipartite subgraph decomposition problem that provides us with a disjoint collection of bipartite subgraphs whose union is  $G$ . A wavelet filterbank can be constructed on each of these subgraphs leading to a multi-dimensional separable wavelet filterbank on any arbitrary graph. Finally, we propose a multi-resolution implementation in which the proposed filterbanks can be recursively applied to the downsampled output coefficients of each channel.

#### A. Downsampling in bipartite graphs

A bipartite graph  $G = (L, H, E)$  is a graph whose vertices can be divided into two disjoint sets  $L$  and  $H$ , such that every link connects a vertex in  $L$  to one in  $H$ . Bipartite graphs are also known as *two-colorable graphs* since the vertices can be colored perfectly into two colors so that no two connected vertices are of the same color. Examples of bipartite graphs include tree graphs, cycle graphs and planar graphs with even degrees. In our analysis, we use the normalized form of the Laplacian matrix  $\mathcal{L} = \mathbf{D}^{-1/2} \mathbf{L} \mathbf{D}^{-1/2}$  for the bipartite graph, which in the case of regular graphs has the same set of eigenvectors as  $\mathbf{L}$ . The normalization reweighs the edges of graph  $G$  so that the degree of each node is equal to 1. To understand the spectral interpretation of  $DU$  operations in bipartite graphs, the following properties of bipartite graphs are useful:

*Lemma 1 ([17, Lemma 1.8]):* The following statements are equivalent for any graph  $G$ :

- 1)  $G$  is bipartite with bipartitions  $H$  and  $L$ .
- 2) The spectrum of  $\mathcal{L}(G)$  is symmetric about 1 and the minimum and maximum eigenvalues of  $\mathcal{L}(G)$  are 0 and 2 respectively.

- 3) If  $\mathbf{u} = \begin{bmatrix} \mathbf{u}_1^T & \mathbf{u}_2^T \end{bmatrix}^T$  is an eigenvector of  $\mathcal{L}$  with eigenvalue  $\lambda$  with  $\mathbf{u}_1$  indexed on  $H$  and  $\mathbf{u}_2$  indexed on  $L$  (or vice-versa) then the deformed eigenvector  $\hat{\mathbf{u}} = \begin{bmatrix} \mathbf{u}_1^T & -\mathbf{u}_2^T \end{bmatrix}^T$  is also an eigenvector of  $\mathcal{L}$  with eigenvalue  $2 - \lambda$ .

Based on these properties of bipartite graphs we state our key result below:

*Proposition 1:* Given a bipartite graph  $G = (L, H, E)$  with Laplacian matrix  $\mathcal{L}$ , if we choose downsampling function  $\beta$  as  $\beta_H$  or  $\beta_L$  as defined in (6), and if  $\mathbf{P}_\lambda$  is the eigen-space corresponding to the eigenvalue  $\lambda_s$  then

$$\mathbf{J}_\beta \mathbf{P}_\lambda = \mathbf{P}_{2-\lambda} \mathbf{J}_\beta. \quad (22)$$

Alternatively, if  $\mathbf{u}_\lambda$  is an eigen-vector of  $\mathcal{L}$  with eigenvalue  $\lambda$  then  $\mathbf{J}_\beta \mathbf{u}_\lambda$  is also an eigen-vector of  $\mathcal{L}$  with eigen-value  $2 - \lambda$ .

*Proof:* Let  $\lambda$  be an eigenvalue of  $G$  with multiplicity  $k$ . This implies that there exists an orthogonal set of  $k$  eigenvectors  $\{\mathbf{u}_i\}_{\lambda_i=\lambda}$  of Laplacian matrix  $\mathcal{L}$  with eigenvalue  $\lambda$ . The projection matrix  $\mathbf{P}_\lambda$  corresponding to  $\lambda$  is given by  $\mathbf{P}_\lambda = \sum_{\lambda_i=\lambda} \mathbf{u}_i \cdot \mathbf{u}_i^t$ . Note that in case of  $k > 1$ , the eigenspace  $\mathbf{P}_\lambda$  is still unique whereas the eigenvectors  $\{\mathbf{u}_i\}_{\lambda_i=\lambda}$  are only unique up to a unitary transformation. If the downsampling function  $\beta$  is chosen as  $\beta_H$  or  $\beta_L$ , then the deformed eigenvector  $\hat{\mathbf{u}}$  in Lemma 1 is equal to  $\mathbf{J}_\beta \mathbf{u}$ , which is an eigen-vector of  $\mathcal{L}$  with eigen-value  $2 - \lambda$ . It can also be seen that if eigenvectors  $\{\mathbf{u}_i\}_{\lambda_i=\lambda}$  are orthogonal to each other then so are the deformed set of eigenvectors  $\{\mathbf{J}_\beta \mathbf{u}_i\}_{\lambda_i=\lambda}$  and form basis of eigenspace  $\mathbf{P}_{2-\lambda}$ . Therefore,  $\mathcal{L} \mathbf{J}_\beta \mathbf{P}_\lambda \mathbf{J}_\beta = \sum_{\lambda_i=\lambda} \mathcal{L} \cdot \mathbf{J}_\beta \mathbf{u}_i \cdot (\mathbf{J}_\beta \mathbf{u}_i)^t = \sum_{\lambda_i=\lambda} (2 - \lambda) \cdot \mathbf{J}_\beta \mathbf{u}_i \cdot (\mathbf{J}_\beta \mathbf{u}_i)^t = (2 - \lambda) \mathbf{P}_{2-\lambda}$ , therefore  $\mathbf{J}_\beta \mathbf{P}_\lambda \mathbf{J}_\beta = \mathbf{P}_{2-\lambda}$  which implies that  $\mathbf{J}_\beta \mathbf{P}_\lambda = \mathbf{P}_{2-\lambda} \mathbf{J}_\beta$ . ■

We term this phenomenon, *spectrum folding* in bipartite graphs, as the deformed eigenvector (or eigenspace) for any  $\lambda \in \sigma(G)$  appears as another eigenvector (or eigenspace) at a mirror eigenvalue around  $\lambda = 1$ . To understand it, let  $\mathbf{f}$  be an  $N$ -D graph-signal on bipartite graph  $G = (L, H, E)$  with eigenspace decomposition

$$\mathbf{f} = \sum_{\lambda \in \sigma(G)} \mathbf{P}_\lambda \mathbf{f} = \sum_{\lambda \in \sigma(G)} \mathbf{f}^\lambda, \quad (23)$$

where  $\mathbf{f}^\lambda = \mathbf{P}_\lambda \mathbf{f}$  is the projection of  $\mathbf{f}$  onto the eigenspace  $V_\lambda$  and let the output signal after  $DU$  operation with downsampling function  $\beta_L$  (or  $\beta_H$ ) be  $\mathbf{f}_{du}$ . Then the  $V_\lambda$  eigenspace projection of the output signal is given as:

$$\mathbf{f}_{du}^\lambda = \mathbf{P}_\lambda \mathbf{f}_{du} = \frac{1}{2} \mathbf{P}_\lambda \mathbf{f} + \mathbf{P}_\lambda \mathbf{J}_{\beta_L} \mathbf{f}, \quad (24)$$

which using (22), can be written as:

$$\begin{aligned}\mathbf{f}_{du}^\lambda &= \frac{1}{2}\mathbf{P}_\lambda\mathbf{f} + \mathbf{J}_{\beta_L}\mathbf{P}_{2-\lambda}\mathbf{f} \\ &= \frac{1}{2}(\mathbf{f}^\lambda + \mathbf{J}_{\beta_L}\mathbf{f}^{2-\lambda}).\end{aligned}\quad (25)$$

In (25), the distortion term  $\mathbf{J}_{\beta_L}\mathbf{f}^{2-\lambda}$ , which arises due to the downsampling of  $\mathbf{f}^\lambda$  has the same coefficients as that of  $\mathbf{f}^{2-\lambda}$  (except for different signs). Further, the eigenspace decomposition of the output signal can be written as:

$$\mathbf{f}_{du} = \frac{1}{2} \sum_{\lambda \in \sigma(G)} (\mathbf{f}^\lambda + \mathbf{J}_\beta \mathbf{f}^{2-\lambda}) = \frac{1}{2}(\mathbf{f} + \mathbf{f}^{alias}) \quad (26)$$

*In other words, the output signal is the average of the original signal and a shifted and aliased version of the original signal, and hence the term spectral folding. In the next Section, we utilize this property to design perfect reconstruction filterbanks for bipartite graphs.*

### B. Two-Channel Filterbank Conditions for Bipartite Graphs

Referring again to Figure 1, for bipartite graph  $G = (L, H, E)$ , let  $\beta_H = \beta$  be the downsampling function for  $\mathbf{H}_1$  filter channel and  $\beta_L = -\beta$  be the downsampling function for  $\mathbf{H}_0$  channel. Thus the nodes in  $H$  only retain the output of highpass channel and nodes in  $L$  retain the output of the lowpass channel. In our proposed design, we also choose the synthesis filters  $\mathbf{G}_0$  and  $\mathbf{G}_1$  to be spectral filters with kernels  $g_0(\lambda)$  and  $g_1(\lambda)$  respectively<sup>3</sup>. Then, by using (5) and (21) the perfect reconstruction conditions in (13) can be rewritten as:

$$\begin{aligned}\mathbf{T}_{eq} &= \mathbf{G}_0\mathbf{H}_0 + \mathbf{G}_1\mathbf{H}_1 \\ &= \sum_{\lambda \in \sigma(G)} (g_0(\lambda)h_0(\lambda) + g_1(\lambda)h_1(\lambda))\mathbf{P}_\lambda \\ \mathbf{T}_{alias} &= \mathbf{G}_1\mathbf{J}_\beta\mathbf{H}_1 - \mathbf{G}_0\mathbf{J}_\beta\mathbf{H}_0 \\ &= \sum_{\lambda, \gamma \in \sigma(G)} (g_1(\lambda)h_1(\gamma) - g_0(\lambda)h_0(\gamma))\mathbf{P}_\lambda\mathbf{J}_\beta\mathbf{P}_\gamma.\end{aligned}\quad (27)$$

<sup>3</sup>In general, synthesis filters do not have to be based on the spectral design. A case is presented in our previous work [18] with linear kernel spectral analysis filters and non-spectral synthesis filters.

1) *Aliasing cancellation*: Using (5) and the spectral folding property of bipartite graphs in (22),  $\mathbf{T}_{alias}\mathbf{f}$  can be written as:

$$\begin{aligned}\mathbf{T}_{alias}\mathbf{f} &= \sum_{\lambda \in \sigma(G)} (g_1(\lambda)h_1(2-\lambda) - g_0(\lambda)h_0(2-\lambda)) \mathbf{J}_\beta \mathbf{P}_{2-\lambda} \mathbf{f} \\ &= \sum_{\lambda \in \sigma(G)} (g_1(\lambda)h_1(2-\lambda) - g_0(\lambda)h_0(2-\lambda)) \mathbf{P}_\lambda \mathbf{J}_\beta \mathbf{f}^{2-\lambda}\end{aligned}\quad (28)$$

Since,  $\mathbf{J}_\beta \mathbf{f}^{2-\lambda}$  is the aliasing term corresponding to  $\mathbf{f}^\lambda$ ,  $\mathbf{T}_{alias}\mathbf{f}$  is the aliasing part of the reconstructed signal, and an *alias-free reconstruction using spectral filters is possible if and only if* for all  $\lambda$  in  $\sigma(G)$ ,

$$g_0(\lambda)h_0(2-\lambda) - g_1(\lambda)h_1(2-\lambda) = 0. \quad (29)$$

2) *Perfect reconstruction*: Perfect reconstruction means that the reconstructed signal  $\hat{\mathbf{f}}$  is the same as (or possibly a scaled version of) the input signal  $\mathbf{f}$ .  $\mathbf{T}_{eq} + \mathbf{T}_{alias} = \mathbf{I}$ . Therefore assuming the filterbanks cancel aliasing, *the perfect reconstruction can be obtained if and only if*  $\mathbf{T}_{eq} = c^2\mathbf{I}$  for some scalar constant  $c$ . Thus, a necessary and sufficient condition for *perfect reconstruction*, using spectral filters, in bipartite graphs filterbanks is that for all  $\lambda$  in  $\sigma(G)$ ,

$$\begin{aligned}g_0(\lambda)h_0(\lambda) + g_1(\lambda)h_1(\lambda) &= c^2, \\ g_0(\lambda)h_0(2-\lambda) - g_1(\lambda)h_1(2-\lambda) &= 0.\end{aligned}\quad (30)$$

3) *Orthogonality*: The equivalent analysis filter  $\mathbf{T}_a$  in the filterbank of Figure 1 is given as

$$\begin{aligned}\mathbf{T}_a &= \frac{1}{2} ((\mathbf{I} - \mathbf{J}_\beta)\mathbf{H}_0 + (\mathbf{I} + \mathbf{J}_\beta)\mathbf{H}_1) \\ &= \frac{1}{2}(\mathbf{H}_0 + \mathbf{H}_1) + \frac{1}{2}\mathbf{J}_\beta(\mathbf{H}_1 - \mathbf{H}_0)\end{aligned}\quad (31)$$

The filterbank provides an *orthogonal decomposition* of the graph signal if  $\mathbf{T}_a^{-1} = \mathbf{T}_a^t$ , which implies  $\mathbf{T}_a\mathbf{T}_a^t = \mathbf{T}_a^t\mathbf{T}_a = \mathbf{I}$ . Since, the spectral filters as well as the downsampling matrix  $\mathbf{J}_\beta$  are symmetric,  $\mathbf{T}_a^t\mathbf{T}_a$  can be expanded as:

$$\mathbf{T}_a^t\mathbf{T}_a = \frac{1}{2} (\mathbf{H}_0^2 + \mathbf{H}_1^2 + \mathbf{H}_1\mathbf{J}_\beta\mathbf{H}_1 - \mathbf{H}_0\mathbf{J}_\beta\mathbf{H}_0) \quad (32)$$



Combining (21) and (32) we obtain:

$$\begin{aligned} \mathbf{T}_a^t \mathbf{T}_a &= 1/2 \sum_{\lambda \in \sigma(G)} \underbrace{(h_0^2(\lambda) + h_1^2(\lambda))}_{C_\lambda} \mathbf{P}_\lambda \\ &+ 1/2 \sum_{\lambda \in \sigma(G)} \underbrace{(h_1(\lambda)h_1(2-\lambda) - h_0(\lambda)h_0(2-\lambda))}_{D_\lambda} \mathbf{J}_\beta \mathbf{P}_\lambda \end{aligned} \quad (33)$$

Thus, orthogonality can be obtained if and only if  $C_\lambda \mathbf{I} + D_\lambda \mathbf{J}_\beta = c^2 \mathbf{I}$  for some constant  $c$  and for all  $\lambda \in \sigma(G)$ , which is possible if and only if  $D_\lambda = 0$  and  $C_\lambda = c^2$  for all  $\lambda$ . Thus, a necessary and sufficient condition for orthogonality in bipartite graph filterbanks using spectral filters is :

$$\begin{aligned} h_0(\lambda)h_0(2-\lambda) - h_1(\lambda)h_1(2-\lambda) &= 0 \\ h_0^2(\lambda) + h_1^2(\lambda) &= c^2. \end{aligned} \quad (34)$$

Note that, comparing (30) and (34), the orthogonality conditions can be obtained from the perfect reconstruction conditions by selecting  $g_0(\lambda) = h_0(\lambda)$  and  $g_1(\lambda) = h_1(\lambda)$ . This is analogous to the case of standard filterbanks and leads to our proposed graph-QMF design as explained in the next Section.

### C. Proposed Solution: Graph-QMF Design

We extend the well-known quadrature mirror filter (QMF) solution to the case of bipartite graphs. Our proposed solution, termed as graph-QMF, leads to the design of a single spectral kernel  $h_0(\lambda)$  by selecting the other spectral kernels as:

$$\begin{aligned} h_1(\lambda) &= h_0(2-\lambda) \\ g_0(\lambda) &= h_0(\lambda) \\ g_1(\lambda) &= h_1(\lambda) = h_0(2-\lambda) \end{aligned} \quad (35)$$

*Proposition 2 (QMF Filters on Graph):* For a bipartite graph  $G = (L, H, E)$ , let a two-channel filterbank be as shown in Figure 1 with the downsampling function  $\beta = \beta_H$  and with spectral filters  $\{\mathbf{H}_0, \mathbf{H}_1, \mathbf{G}_0, \mathbf{G}_1\}$  corresponding to spectral kernels  $\{h_0(\lambda), h_1(\lambda), g_0(\lambda), g_1(\lambda)\}$  respectively. Then for any arbitrary choice of kernel  $h_0(\lambda)$ , the proposed graph-QMF solution cancels aliasing in the filterbank. In addition for  $h_0(\lambda)^2 + h_0(2-\lambda)^2 = c^2$  for all  $\lambda \in \sigma(G)$  and  $c \neq 0$  the filterbank provides perfect reconstruction and an orthogonal decomposition of graph-signals.

*Proof:* Substituting (35) into (29) leads to  $g_0(\lambda)h_0(2-\lambda) - g_1(\lambda)h_1(2-\lambda) = 0$  and aliasing is indeed canceled. The reconstructed signal  $\hat{\mathbf{x}}$  in this case is simply equal to  $(1/2)\mathbf{T}_{eq}\mathbf{x}$  and can be written

as:

$$\hat{\mathbf{x}} = \frac{1}{2} \sum_{\lambda \in \sigma(G)} (h^2(\lambda) + h^2(2 - \lambda)) \mathbf{x}^\lambda \quad (36)$$

Thus for  $(h^2(\lambda) + h^2(2 - \lambda)) = c^2$  and  $c \neq 0$ , the reconstructed signal  $\hat{\mathbf{x}} = \frac{c^2}{2} \mathbf{x}$  is a scaled version of original signal. Similarly applying the mirror design  $h_1(\lambda) = h_0(2 - \lambda)$  in the conditions (34) we get  $h_0(\lambda)h_0(2 - \lambda) - h_1(\lambda)h_1(2 - \lambda) = 0$  and  $h_0^2(\lambda) + h_1^2(\lambda) = c^2$  and hence corresponding analysis side transform  $\mathbf{T}_a$  is orthogonal. ■

We now consider the design of kernels  $h_0(\lambda)$  satisfying the design constraint of Proposition 2, i.e., for which  $h_0^2(\lambda) + h_0^2(2 - \lambda) = c^2$  for all  $\lambda \in \sigma(G)$ . For maximum spectrum splitting in the two channels of the filterbank, the ideal choice of kernel  $h_0(\lambda)$  would be a lowpass rectangular function on  $\lambda$  given as:

$$h_0^{ideal}(\lambda) = \begin{cases} c & \text{if } \lambda < 1 \\ c/\sqrt{2} & \text{if } \lambda = 1 \\ 0 & \text{if } \lambda > 1 \end{cases} \quad (37)$$

The corresponding ideal filter is given by

$$\mathbf{H}_0^{ideal} = \sum_{\lambda < 1} c \mathbf{P}_\lambda + \frac{c}{\sqrt{2}} \mathbf{P}_{\lambda=1} \quad (38)$$

Note that the ideal transform has a non-analytic spectral kernel response with sharp peaks and is therefore a global transform (i.e., the filter operations are not localized). Even analytic solutions of the constraint equation  $h_0^2(\lambda) + h_0^2(2 - \lambda) = c^2$ , such as  $h_0(\lambda) = c\sqrt{1 - \lambda/2}$  or  $h_0(\lambda) = c \cos(\pi\lambda/4)$ , are not very well localized in the spatial domain. By relaxing the constraints one can obtain spatially localized solutions at the cost of some small reconstruction error and near-perfect orthogonality. One such solution is the approximation of the desired kernel with a polynomial kernel. We choose polynomial approximations of the desired kernel due to the following localization property for corresponding transforms:

*Lemma 2 ([8]):* Let  $h_0(\lambda)$  be a polynomial of degree  $k$  and let  $\mathcal{L}$  be the normalized Laplacian matrix for any weighted graph  $G$ , then the matrix polynomial  $\mathbf{H}_0 = h_0(\mathcal{L})$  is exactly  $k$ -hop localized at each node of  $G$ . In other words for any two nodes  $n$  and  $m$  if  $m \notin \mathcal{N}_k(n)$  then  $\mathbf{H}_0(n, m) = 0$ .

Further, we choose a minimax polynomial approximation which minimizes the Chebychev norm (worst-case norm) of the reconstruction error since it has been shown in [8] that it also minimizes the upper-bound on the error  $\|H^{ideal} - H^{poly}\|$  between ideal and approximated filters. Thus, in order to localize the filters on the graph, we approximate  $h_0^{ideal}$  with the truncated Chebychev polynomials (which are a good approximation of minimax polynomials) of different orders. However since  $h_0^{ideal}$  is a rectangular

function it projects a lot of its energy in the truncated part of the polynomial expansions and as a result the polynomial approximation errors for  $h_0^{ideal}$  are high. A possible solution of this problem is to soften the ideal case, by finding a smooth function that is low-pass and satisfies the constraint. An analogous construction in regular signal processing is *Meyer's wavelet* design which replaces the brick-wall type ideal frequency-response with a smooth scaling function that satisfies the orthogonality and scaling requirements. By a change in variable from  $\omega \in [-1, 1]$  to  $\lambda \in [0, 2]$  we can extend Meyer's wavelet construction in the case of bipartite graph. The construction involves choosing a function  $\nu(x)$  such that  $\nu(\lambda) = 0$  for  $\lambda \leq 0$ ,  $\nu(\lambda) = 1$  for  $\lambda \geq 1$  and  $\nu(\lambda) + \nu(1 - \lambda) = 1$  everywhere. One such function is given as:

$$\nu(\lambda) = \begin{cases} 1 & \text{if } \lambda \leq 0 \\ 3\lambda^2 - 2\lambda^3 & \text{if } 0 \leq \lambda \leq 1 \\ 0 & \text{if } 1 \geq \lambda \end{cases} \quad (39)$$

The smooth kernel is then given as:

$$h_0^{Meyer}(\lambda) = \sqrt{\nu(2 - \frac{3}{2}\lambda)} \quad (40)$$

In Figure 2(a), we plot the ideal and Meyer wavelet kernels and in Figures 2(b)-(f) we plot the reconstruction errors between desired kernels and their polynomial approximations of different orders. It can

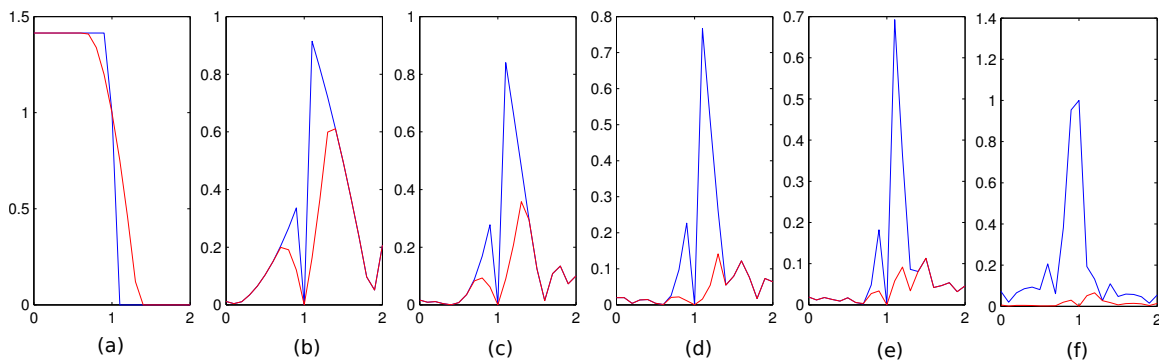


Fig. 2: (a) Ideal kernel (blue) vs. Meyer's wavelet kernel (red). It can be seen that Meyer's wavelet has smoother transition at  $\lambda = 1$  than the ideal kernel, (b)-(f) the reconstruction error magnitudes between original kernels and their polynomial approximations of order 2, 4, 6, 8 and 10 respectively: ideal kernel (blue curves) and Meyers kernel (red curve).

be seen that Meyer's wavelet approximations yield small reconstruction errors as compared to ideal-filter approximations. Thus by choosing  $h(\lambda)$  as the low-order polynomial approximations of smooth low-pass functions (such as Meyer's wavelets), we obtain near perfect reconstruction QMF wavelet filters on any bipartite graph which are very well localized in spatial domain.

#### D. Multi-dimensional separable wavelet filterbanks for arbitrary graphs

Not all graphs are bipartite. In order to apply our filterbank design to an arbitrary graph,  $G = (\mathcal{V}, E)$ , we propose a *separable downsampling and filtering* approach, where our previously designed two-channel filterbanks are applied in a “cascaded” manner, by filtering along a series of bipartite subgraphs of the original graph. This is illustrated in Figure 3. We call this a “separable” approach in analogy to separable transforms for regular multidimensional signals. For example in the case of separable transforms for 2D signals, filtering in one dimension (e.g., row-wise) is followed by filtering of the outputs along the second dimension (column-wise). In our proposed approach, a stage of filtering along one “dimension” corresponds to filtering using *only* those edges that belong to the corresponding bipartite subgraph. As shown in Figure 3, after filtering along one subgraph the results are stored in the vertices, and a new transform is applied to the resulting graph signals following the edges of the next level bipartite subgraph.

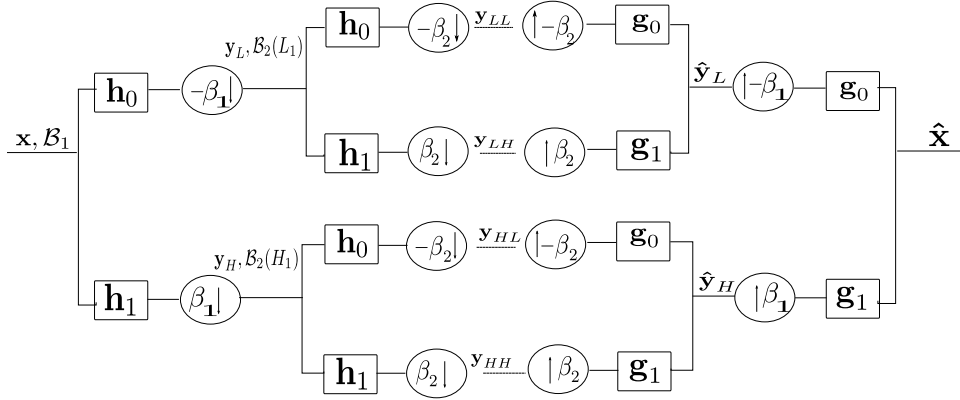


Fig. 3: Block diagram of a 2D Separable two-channel Filter Bank: the graph  $G$  is first decomposed into two bipartite subgraphs  $\mathcal{B}_1$  and  $\mathcal{B}_2$ , using the proposed decomposition scheme. The first two-channel filterbank is designed on  $\mathcal{B}_1$ . The filtering and downsampling on  $\mathcal{B}_1$  creates output coefficients  $y_H$  and  $y_L$ , stored on the sets  $H_1$  and  $L_1$ , respectively. The second filterbank is designed on  $\mathcal{B}_2$ , which operates separately on signals  $y_H$  and  $y_L$  using the links of bipartite subgraphs  $\mathcal{B}_2(H_1)$  and  $\mathcal{B}_2(L_1)$  respectively. This creates 4 sets of output transform coefficients, denoted as  $y_{HH}, y_{HL}, y_{LH}$  and  $y_{LL}$ , which are stored at disjoint sets of nodes, given as  $H_1 \cap H_2, H_1 \cap L_2, L_1 \cap H_2$  and  $L_1 \cap L_2$ , respectively.

In what follows we will assume that  $G$  has been decomposed into a series of  $K$  bipartite subgraphs  $\mathcal{B}_i = (L_i, H_i, E_i)$ ,  $i = 1 \dots K$ ; how such a decomposition may be obtained will be discussed later. The bipartite subgraphs cover the same vertex set:  $L_i \cup H_i = \mathcal{V}$ ,  $i = 1, 2, \dots, K$ . Each edge in  $G$  belongs to exactly one  $E_i$ , i.e.,  $E_i \cap E_j = \emptyset$ ,  $i \neq j$ ,  $\bigcup_i E_i = E$ . Note that in each bipartition we need to decide both a 2-coloring  $(H_i, L_i)$  and an assignment of edges  $(E_i)$ . In order to guarantee invertibility for structures such as those of Figure 3, given the chosen 2-colorings  $(H_i, L_i)$ , the edge assignment has to be performed iteratively based on the order of the subgraphs. That is, edges for subgraph 1 are chosen first, then those for subgraph 2 are selected, and so on. The basic idea is that at each stage  $i$  all edges between vertices of

different colors *that have not been assigned yet* will be included in  $E_i$ . More formally, at stage  $i$  with sets  $H_i$  and  $L_i$ ,  $E_i$  contains *all* the links in  $E - \bigcup_{k=1}^{i-1} E_k$  that connect vertices in  $L_i$  to vertices in  $H_i$ . Thus  $E_1$  will contain all edges between  $H_1$  and  $L_1$ . Then, we will assign to  $E_2$  all the links between nodes in  $H_2$  and  $L_2$  that were not already in  $E_1$ . This is also illustrated in Figure 4. Note that, by construction  $G_1 = G - \mathcal{B}_1 = (\mathcal{V}, E - E_1)$  contains now two disjoint graphs, since all edges between  $L_1$  and  $H_1$  were assigned to  $E_1$ . Thus, at the second stage in Figure 3,  $\mathcal{B}_2$  is composed of two disjoint graphs  $\mathcal{B}_2(L_1)$  and  $\mathcal{B}_2(H_1)$ , which each will be processed independently by one of the two filterbanks at this second stage. Clearly, this guarantees invertibility of the decomposition of Figure 3, since it will be possible to recover the signals in  $\mathcal{B}_2(L_1)$  and  $\mathcal{B}_2(H_1)$  from the outputs of the 2nd stage of the decomposition. The same argument can be applied to the decompositions with more than two stages. That is, the output of a two-channel filterbank at level  $i$  leads to two subgraphs, one per channel, that are disconnected when considering the remaining edges  $(E - \bigcup_{k=1}^i E_k)$ . The output of a  $K$ -level decomposition leads to  $2^K$  disconnected subgraphs.

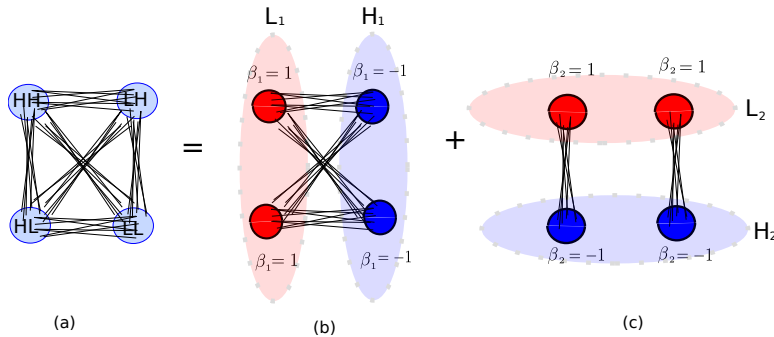


Fig. 4: Example of 2-dimensional separable downsampling on a graph: (a) original graph  $G$ , (b) the first bipartite graph  $\mathcal{B}_1 = (L_1, H_1, E_1)$ , containing *all* the links in  $G$  between sets  $L_1$  and  $H_1$ . (c) the second bipartite graph  $\mathcal{B}_2 = (L_2, H_2, E_2)$ , containing *all* the links in  $G - \mathcal{B}_1$ , between sets  $L_2$  and  $H_2$

We now derive expressions for the proposed cascaded transform along bipartite subgraphs. Using  $K = 2$  case as an example, assuming that the original graph can be approximated exactly with two bipartite subgraphs as shown in Figure 4, we choose  $\beta_i = \beta_{H_i}$  as the downsampling function for bipartite graph  $\mathcal{B}_i$ , for  $i = 1, 2$ . Further, let us denote  $\mathbf{J}_{\beta_i}$ , as the downsampling matrices, and  $\mathbf{H}_{i0}$  and  $\mathbf{H}_{i1}$  as the low-pass and high-pass graph-QMF filters respectively, for the bipartite graph  $\mathcal{B}_i$ , for  $i = 1, 2$ . Since, the vertex sets  $L_1$  and  $H_1$  in bipartite graph  $\mathcal{B}_2$  are disconnected, the filtering and downsampling operations on graphs  $\mathcal{B}_2(L_1)$  and  $\mathcal{B}_2(H_1)$  do not interact with each other. Therefore, graph-filters  $\mathbf{H}_{2j}$ , for  $j = 0, 1$  on the second bipartite graph  $\mathcal{B}_2$ , can be represented as *block-diagonal matrices* with diagonal entries  $\mathbf{H}_{2j}(H_1, H_1)$  and  $\mathbf{H}_{2j}(L_1, L_1)$ . As a result,  $\mathbf{H}_{20}$  and  $\mathbf{H}_{21}$  commute with downsampling matrix  $\mathbf{J}_{\beta_1}$  of

the first bipartite subgraph, i.e.,

$$\mathbf{H}_{2j}\mathbf{J}_{\beta_1} = \mathbf{J}_{\beta_1}\mathbf{H}_{2j}, \quad (41)$$

for  $j = 1, 2$ .<sup>4</sup> Further, let  $\mathbf{T}_{ai}$  be the equivalent analysis transform for  $\mathcal{B}_i$ , for  $i = 1, 2$ . The combined analysis transform  $\mathbf{T}_a$  in the 2-dimensions can be written as the product of analysis transform in each dimension. Using (31), we obtain:

$$\mathbf{T}_a = \mathbf{T}_{a2} \cdot \mathbf{T}_{a1} = \prod_{i=1}^2 \frac{1}{2} ((\mathbf{H}_{i1} + \mathbf{H}_{i0}) + \mathbf{J}_{\beta_i}(\mathbf{H}_{i1} - \mathbf{H}_{i0})), \quad (42)$$

Note that, for exact graph-QMF filter design such as with the Meyer kernel in (40),  $\mathbf{T}_{ai}$  is invertible with  $\mathbf{T}_{ai}^{-1} = \mathbf{T}_{ai}^t$ , for  $i = 0, 1$ . As a result,  $\mathbf{T}_a$  is invertible with  $\mathbf{T}_a^{-1} = \mathbf{T}_{a1}^t \cdot \mathbf{T}_{a2}^t$ .<sup>5</sup> The transform function  $\mathbf{T}_a$  can be further decomposed into the transform functions  $\mathbf{T}_{HH}$ ,  $\mathbf{T}_{Hl}$ ,  $\mathbf{T}_{LH}$  and  $\mathbf{T}_{LL}$  corresponding to the four channels in Figure 3. For example, the transform  $\mathbf{T}_{HH}$ , consists of all the terms in the expansion of  $\mathbf{T}_a$  in (42), containing filters  $H_{11}$  and  $H_{21}$ . Thus,

$$\mathbf{T}_{HH} = \frac{1}{4}(\mathbf{H}_{21}\mathbf{H}_{11} + \mathbf{H}_{21}\mathbf{J}_{\beta_1}\mathbf{H}_{11} + \mathbf{J}_{\beta_2}\mathbf{H}_{21}\mathbf{H}_{11} + \mathbf{J}_{\beta_2}\mathbf{H}_{21}\mathbf{J}_{\beta_1}\mathbf{H}_{11}), \quad (43)$$

where  $(1/4)\mathbf{H}_{21}\mathbf{H}_{11}$  is the transform without downsampling, and the remaining terms arise primarily due to the downsampling in the  $HH$  channel. Using (41), which is a property of our proposed decomposition scheme in (43), we obtain:

$$\begin{aligned} \mathbf{T}_{HH} &= \frac{1}{4}(\mathbf{H}_{21}\mathbf{H}_{11} + \mathbf{J}_{\beta_1}\mathbf{H}_{21}\mathbf{H}_{11} + \mathbf{J}_{\beta_2}\mathbf{H}_{21}\mathbf{H}_{11} + \mathbf{J}_{\beta_2}\mathbf{J}_{\beta_1}\mathbf{H}_{21}\mathbf{H}_{11}) \\ &= \frac{1}{4}(\mathbf{I} + \mathbf{J}_{\beta_2})(\mathbf{I} + \mathbf{J}_{\beta_1})\mathbf{H}_{21}\mathbf{H}_{11}. \end{aligned} \quad (44)$$

Thus, the equivalent transform in each channel of the proposed 2-dimensional separable filterbanks can be interpreted as filtering with a 2-dimensional filter, such as  $\mathbf{H}_{21}\mathbf{H}_{11}$  for the  $HH$  channel, followed by  $DU$  operations with two downsampling functions  $\beta_2(n)$  and  $\beta_1(n)$  in cascade. It also follows from (44), that the output of  $\mathbf{H}_{21}\mathbf{H}_{11}$  in the  $HH$  channel is stored only at the nodes corresponding to  $H_1 \cap H_2$ . Thus, the output of each channel is stored at mutually disjoint sets of nodes, and each node stores the output of exactly one of the channel. Therefore, the overall filterbank is *critically sampled*. Further, if the spectral decompositions of  $\mathcal{B}_1$  and  $\mathcal{B}_2$  are given as  $\{\lambda, \mathbf{P}_\lambda^1\}$  and  $\{\gamma, \mathbf{P}_\gamma^2\}$ , then  $\mathbf{H}_{21}\mathbf{H}_{11}$  consists of a two

<sup>4</sup>In general, this result can be applied to any general  $K$ -dimensional decomposition using proposed recursive method, as the downsampling matrix  $\mathbf{J}_{\beta_i}$  commutes with all filter matrices  $\mathbf{H}_{k1}$  and  $\mathbf{H}_{k2}$  corresponding to bipartite subgraph  $\mathcal{B}_k$ , where  $k > i$ .

<sup>5</sup>For polynomial approximations, of Meyer kernels, we incur some reconstruction errors in each dimension.

dimensional spectral kernel  $h_{21}(\gamma)h_{11}(\lambda)$  and corresponding eigenspace  $\mathbf{P}_\gamma^2\mathbf{P}_\lambda^1$ . The analysis extends to any dimension  $K > 2$  with  $K$ -dimensional graph-frequencies  $(\lambda_1, \lambda_2, \dots, \lambda_K)$ , corresponding eigenspace  $\mathbf{P}_{\lambda_1}^1, \mathbf{P}_{\lambda_2}^2, \dots, \mathbf{P}_{\lambda_K}^K$  and transforms with spectral response  $\prod_{i=1}^K g_i(\lambda_i)$ .

So far we have described, how to implement separable multi-dimensional graph-QMF filterbanks on a graph  $G$ , given a decomposition of  $G$  into  $K$  bipartite subgraphs. In particular, we defined a ‘‘separable’’ method of graph decomposition, which leads to a cascaded tree-structured implementation of the multi-dimensional filterbanks. While these multi-dimensional filterbanks can be implemented for *any* separable bipartite subgraph decomposition of  $G$ , the definition of a ‘‘good’’ bipartite decomposition of any arbitrary graph remains a topic for future work, and may be application dependent. In this paper, we propose a bipartite subgraph decomposition method, referred to as *Harary’s decomposition*, which provides a  $\lceil \log_2 k \rceil$  bipartite decomposition of a graph  $G$  given a  $k$ -coloring defined on it<sup>6</sup>. The method is derived from [19] and we describe it in Algorithm 1.<sup>7</sup>

---

**Algorithm 1** Harary’s Decomposition

---

**Require:**  $\mathbf{F}$ , s.t.  $F(v)$  is the color assigned to node  $v$ ,  $\min(F)=1$ ,  $\max(F)=k$ .

- 1: Set  $L_1 =$  set of nodes with  $F(v) \leq \lfloor k/2 \rfloor$  colors.
  - 2: Set  $H_1 =$  set of nodes with  $F(v) > \lfloor k/2 \rfloor$  colors.
  - 3: Set  $E_1 \subset E$  containing all the edges between sets  $H_1$  and  $L_1$ .
  - 4: Compute bipartite subgraph  $\mathcal{B}_1 = (L_1, H_1, E_1)$ ,
  - 5: Set  $G = G - \mathcal{B}_1$ .
  - 6:  $G$  is now a union of two disconnected subgraphs  $G(H_1)$  and  $G(L_1)$ .
  - 7: Graph  $G(L_1)$  is  $\lfloor k/2 \rfloor$ -colorable.
  - 8: Compute coloring  $\mathbf{F}_L$  on  $G(L_1)$  s.t.  $\min(F_L)=1$ ,  $\max(F_L)=\lfloor k/2 \rfloor$ .
  - 9: Graph  $G(H_1)$  is  $\lfloor k/2 \rfloor$ -colorable.
  - 10: Compute coloring  $\mathbf{F}_H$  on  $G(H_1)$  s.t.  $\min(F_H)=1$ ,  $\max(F_L)=\lfloor k/2 \rfloor$ .
  - 11: Repeat 1 – 4 on  $G(L_1)$  and  $G(H_1)$  to obtain bipartite subgraphs  $\mathcal{B}_2(L_1)$  and  $\mathcal{B}_2(H_1)$ .
  - 12: Compute bipartite subgraph  $\mathcal{B}_2 = \mathcal{B}_2(L_1) \cup \mathcal{B}_2(H_1)$ .
  - 13: Set  $G = G - \mathcal{B}_2$ .
  - 14: repeat 1 – 13 exactly  $\lceil \log_2 k \rceil$  times after which graph  $G$  will become an empty graph.
- 

Note that invertible cascaded transforms can also be constructed even when the conditions for edge selection described are not followed, e.g., if an edge  $e_1$  between nodes in  $H_1$  and  $L_1$  is *not* included in  $E_1$ . In such a situation, it is possible to perform an invertible cascaded decomposition if  $e_1$  is no longer used in further stages of decomposition. Thus, we would have an invertible decomposition but on a graph

<sup>6</sup>A graph is perfectly  $k$ -colorable if its vertices can be assigned  $k$ -colors in such a way that no two adjacent vertices share the same color. The term *chromatic number*  $\chi(G)$  of a graph refers to smallest such  $k$ .

<sup>7</sup>Note that the bipartite decomposition is not unique and depends on the ordering in which the  $k$ -colors are divided.

that approximates the original one (i.e., without considering  $e_1$ ). Alternatively it can be shown that it is possible to design invertible transforms with arbitrary  $E_i$  selections (i.e., not following the rules set out in this paper), but these transforms are not necessarily critically sampled. A more detailed study of this case falls outside of the scope of this paper.

#### *E. Multiresolution decomposition using two-channel filterbanks*

The two-channel filterbanks on a single bipartite graph  $\mathcal{B} = (H, L, E)$  have the property of decomposing the signal into two lower-resolution versions  $\hat{\mathbf{f}}_L$  and  $\hat{\mathbf{f}}_H$  respectively, as in (11). The signal  $\hat{\mathbf{f}}_L$  is a lowpass or coarse resolution version constructed from the output coefficients of the lowpass channel stored on the set  $L$ , whereas  $\hat{\mathbf{f}}_H$  is a highpass version of the input constructed from the output coefficients of the filterbank stored on the set  $H$ . Analogous to tree-structured filterbanks for 1-D signals, this decomposition can be applied recursively on the low-pass (or high-pass) signal by constructing a downsampled graph consisting of vertices in  $L$  (or  $H$ ) and some appropriate edge-structure. One way to compute the downsampled graph  $G_L$  (or  $G_H$ ) is to reconnect two nodes in set  $L$  (or  $H$ ) if they are 2-hops away in the original graph. Note that for bipartite graphs, unlike the case of regular lattices, the resulting downsampled graphs  $G_L$  and  $G_H$  may neither be identical nor bipartite. Therefore, for the next level of decomposition, we can either operate on a single bipartite graph approximation of  $G_L$  which leads to a one-dimensional two-channel filterbank, or a multiple bipartite graph approximation, which leads to a multi-dimensional two-channel filterbank implementation on the downsampled graph. Further, this multiresolution decomposition of graph-signals can be extended to the case of general  $K$ -dimensional two-channel filterbanks for any arbitrary graph  $G$ , which decomposes the signal into  $2^K$  lower-resolution versions, as described in Section III-D. In this case, the downsampled graphs in each channel, can be computed by reconnecting two nodes in the downsampled vertex set, if they are  $2^K$ -hops away in the original graph.

## IV. EXPERIMENTS

### *A. Graph-QMF Design Details*

We first provide explicit details of the filterbank design for arbitrary graphs. Given any arbitrary undirected graph  $G = (\mathcal{V}, E)$ , we find a minimum perfect-coloring  $\chi$  of its vertices using a graph-coloring algorithm, such as the BSC algorithm given in [20]. The coloring information is then used to decompose  $G$  into a set of  $K = \lceil \log_2(\chi) \rceil$  bipartite graphs  $\mathcal{B}_i = (L_i, H_i, E_i)$ , for  $i = 1, 2, \dots, K$  using Harary's Algorithm as described in Section III-D. For each subgraph  $\mathcal{B}_i$ , we compute its normalized



Laplacian matrix  $\mathcal{L}_i$  and the downsampling function  $\beta_i = \beta_{H_i}$ . Further, we compute the low-pass analysis kernel  $h_{i,0}(\lambda)$  on  $\mathcal{B}_i$ , as the  $m_i^{\text{th}}$  order Chebychev approximation of the Meyer kernel  $h_0^{\text{Meyer}}(\lambda)$ , for some positive integer value  $m_i$ . The remaining spectral kernels  $h_{i,1}(\lambda), g_{i,0}(\lambda), g_{i,1}(\lambda)$  are computed from  $h_{i,0}(\lambda)$  according to graph-QMF relations mentioned in (35). The corresponding analysis and synthesis transforms are then computed as  $\mathbf{H}_{i,j} = h_j(\mathcal{L}_i)$  and  $\mathbf{G}_{i,j} = g_j(\mathcal{L}_i)$ , respectively, for  $j = 0, 1$ . Note that, since the kernels are polynomials, the transforms are also matrix polynomials of Laplacian matrices and do not require explicit eigenspace decompositions. In our experiments, we use  $m_i = m$ , and hence  $h_{i,j}(\lambda) = h_j(\lambda)$ ,  $j \in \{0, 1\}$  for all  $i$ , in which case the resulting transforms are exactly  $m$ -hop localized on each bipartite subgraph. The order  $m$  is a parameter of our design and should be chosen based on the required level of spatial localization and how much reconstruction error can be tolerated. The overall filterbank is designed by concatenating filterbanks of each bipartite subgraph in the form of a tree, analogous to Figure 3 in the 2-dimensional decomposition case. We now describe some experiments to demonstrate potential applications of our proposed filterbanks.

### B. Graph Filter-banks on Images

Digital images are 2-D regular signals, but they can also be formulated as graphs by connecting every pixel (node) in an image with its neighboring pixels (nodes) and by interpreting pixel values as the values of the graph-signal at each node. The graph-representations of the regular-signals are shown to be promising in practice recently [21], [22]. Figure 5 shows some of the ways in which pixels in an image can be connected with each other to formulate a graph representation of any image. The advantage of using a graph formulation of the images is that it provides flexibility of linking pixels in arbitrary ways, leading to different filtering/downsampling patterns. To demonstrate this, we implement an ideal spectral low-pass

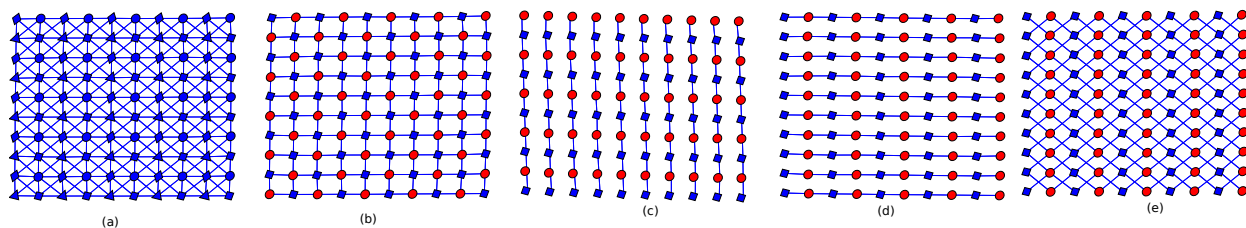


Fig. 5: Some of the graph-formulation of a 2D image lattice: (a) shows an 8-connected image graph  $G$  formed by connecting each pixel with its 8 nearest neighbors. The graph is 4-colorable, and the nodes of different shapes (squares, circles, triangles and diamonds) represent different colors. (b) shows the image-graph  $G^r$  by connecting each pixel with its rectangular (NWSE) neighbors only, (c) the image graph  $G^v$  with vertical links only (d) the image-graph  $G^h$  with horizontal links only. and (e) shows image-graph  $G^d$  with each pixel linked to its 4 diagonal neighbors. The graphs shown in (b), (c), (d) and (e) are bipartite graphs, with the partitions represented as nodes with different colors and shapes (red-circles vs. blue-squares).

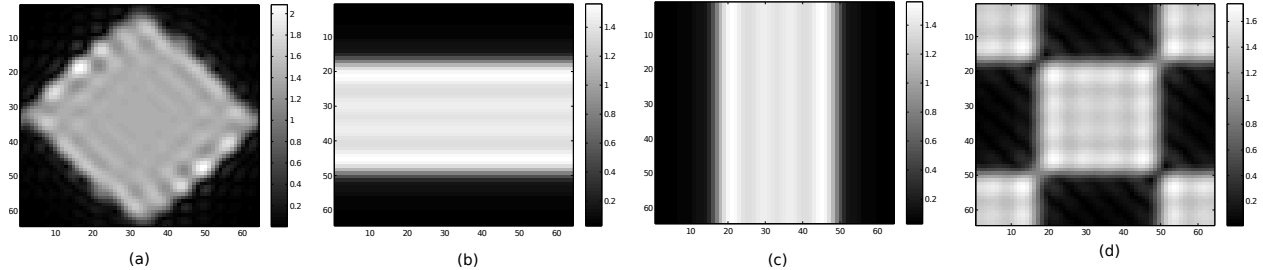


Fig. 6: Discrete Fourier frequency magnitude responses of ideal lowpass filters on some bipartite image-graphs. Fig. (a) ideal lowpass filter response on NWSE bipartite subgraph  $G^r$  shown in 5b, Fig. (b) ideal lowpass filter response on diagonally connected bipartite subgraph  $G^d$  shown in 5c, Fig. (c) ideal lowpass filter on vertical-links only bipartite subgraph shown in 5d, Fig. (d) ideal lowpass filter on horizontal-links only bipartite subgraph shown in 5e.

filters on the graph formulations of the 2D images, shown in Figure 5. Since, the graphs  $G^r$ ,  $G^v$ ,  $G^h$  and  $G^d$  are all bipartite graphs, the ideal spectral lowpass filter  $\mathbf{H}_0^{ideal}$  on these graph can be computed as in (38). In Figure 6, we plot the *DFT* magnitude response of ideal lowpass spectral transforms on bipartite image-graphs  $G^r$ ,  $G^v$ ,  $G^h$  and  $G^d$  respectively.<sup>5</sup> In Figure 5(b) the downsampling pattern (red/blue nodes) on the rectangular subgraph  $G^r$  is identical to the quincunx downsampling pattern, and in Figure 6(a), it can be observed that the DFT magnitude response of the spectral low-pass filter on  $G^r$  is same as the DFT magnitude response of the standard anti-aliasing filter for quincunx downsampling. Similarly, we observe that the spectral low-pass filters for  $G^v$  in Figure 5(c) and  $G^h$  in Figure 5(d) have the same DFT magnitude responses (Figure 6(b) and 6(c)) as the anti-aliasing filters for vertical and horizontal factor-of-2 downsampling cases, respectively. Further, the graph formulation of images allows us to explore new downsampling patterns, for example, the image pixels can be connected to their diagonally opposite neighbors as shown in Figure 5(e). The DFT magnitude response of the ideal spectral low-pass filter in this case, is shown in Figure 6(d) and has a wider passband in the diagonal directions. Further, in the non-bipartite graph formulation of the anti-aliasing filter for any arbitrary graph is the product of ideal-lowpass filters along its bipartite subgraph decompositions. Therefore the rectangular graph  $G^r$  can be further decomposed into bipartite subgraph  $G^v$  and  $G^h$  leading to a rectangular (factor of 4) downsampling pattern.

This graph-based approach also provides additional degrees of freedom (directions) to filter/downsample the image while still having a critically sampled output. To demonstrate this, we implement a graph wavelet filterbank on the 8-connected image-graph  $G$  of a given image. The chromaticity of  $G$  is  $\chi = 4$

<sup>5</sup>Because of the regularity and symmetry of the links, the resulting filters at each node, are translated version of each other (except at the boundary nodes), and so we can compute the 2-D DFT magnitude response of a spectral transform, by computing the DFT response of the filtering operations at a single node.

(represented as different shape nodes in Figure 5(a)) and hence it can be decomposed into two edge-disjoint bipartite subgraphs. Among several such possible decompositions, we choose the decomposition that gives us a rectangular subgraph  $G^r$  and a diagonally connected diamond graph  $G^d$ . On each subgraph we implement a graph-QMF filterbank, as described in Section IV-A above. The resulting 2-dim separable filterbank has four channels as shown in Figure 3 and the nodes representing a specific shape in Figure 5(a) store the output of a specific channel.<sup>6</sup> Figure 7 shows the output wavelet coefficients of proposed 2-dim filterbank on a toy image which has both diagonal and rectangular edges. In Figure 7, the energy of wavelet coefficients in the LH channel (low-pass on  $G^r$ , high-pass on  $G^d$ ) is high around the rectangular edges, which is reasonable, since subgraph  $G^d$  is diagonally connected and its low-pass spectral frequencies are oriented along diagonal links. Similarly we observe that the high-energy wavelet coefficients in the HL channel (high-pass on  $G^r$ , low-pass on  $G^d$ ) lie around the diagonal edges, since  $G^r$  is rectangularly connected and its low-pass spectral frequencies are oriented towards horizontal and vertical directions. This example also shows that the filterbanks based on only NWSE connectivity are more suited for images with horizontal and vertical edges whereas the transform based only on diamond connectivity are more suited for image with diagonal edges. In Figure 8, we show the graph-wavelet decomposition of a depth-map image taken from [23]. Again, we see that the LH channel has high energy coefficients along nearly rectangular edges while the HL channel has high energy coefficients along nearly diagonal directions. More directions can be added to downsample/filter by increasing the connectivity of the pixels in the image-graph. Moreover, since graph-based transforms operate only over the links between nodes, the graph formulation is useful in designing edge-aware transforms, such as [21], [22], (which avoid filtering across edges) by removing links between pixels across edges.

### C. Graph Filter-banks on Irregular Graphs

Our proposed filterbanks can be used as a useful tool in analyzing/compressing arbitrarily linked irregular graphs. In order to demonstrate it we take the example of *Minnesota traffic graph*  $G$  as shown in Figure 9(a). Further, we consider the decomposition of a graph-signal whose scatter-plot is shown in Figure 9(b), using our proposed filterbanks on graph. The graph is perfectly 3-colorable and hence, we can decompose it into  $\lceil \log_2(3) \rceil = 2$  bipartite subgraphs  $\mathcal{B}_1$  and  $\mathcal{B}_2$  which are shown in Figure 10(a) and 10(b) respectively.

<sup>6</sup>In general for an arbitrary graph with  $K$ -proper colors, the bipartite decomposition provides exactly  $K$  non-empty channels and nodes of a particular color store the output of a particular channel.

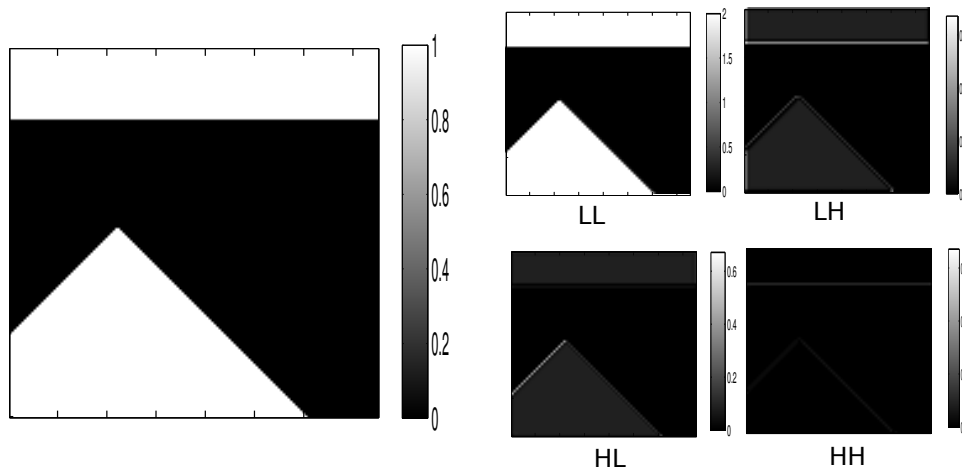


Fig. 7: Separable two-dim two channel graph filterbank on a toy image with both rectangular and diagonal edges. The filterbank is the concatenation of proposed graph-QMF filterbank with  $m = 2$  order approximation of Meyer kernel on subgraph  $G^r$  and subgraph  $G^d$  as shown in Figure 3

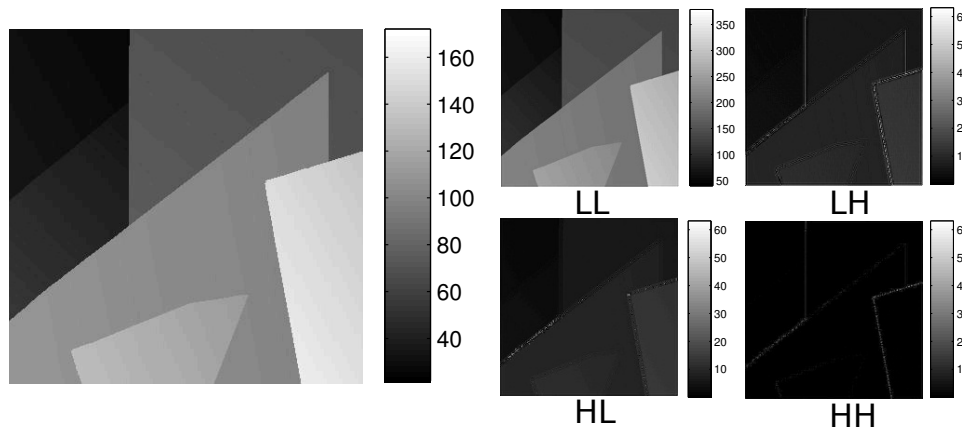


Fig. 8: Separable two-dim two channel graph filterbank on a depth-map image with parameter  $m = 6$

Given such decomposition, we implement a 2-dim separable 2-channel graph-QMF filterbank on the Minnesota graph, with parameter value  $m = 6$ , according to the details given in Section IV-A. Since the proper coloring of graph  $G$  is 3, there are no nodes to sample  $HL$  channel output (i.e. nodes for which  $(\beta_1(n), \beta_2(n)) = (-1, 1)$ ) and hence there are only three non-empty channels ( $LL, LH, HH$ ). Figure 11 shows the output wavelet coefficients. The  $HL$  channel is empty and is not displayed in the results. Due to downsampling, the total number of output coefficients in the four channel is equal to number of input samples, thus making the transform *critically sampled*. We observe in Figure 11 that for the  $LL$  channel  $(\beta_1(n), \beta_2(n)) = (1, 1)$ , the signal on the downsampled graph is a smooth approximation of the original signal (sharp boundaries blurred). The remaining channels store the detail information required

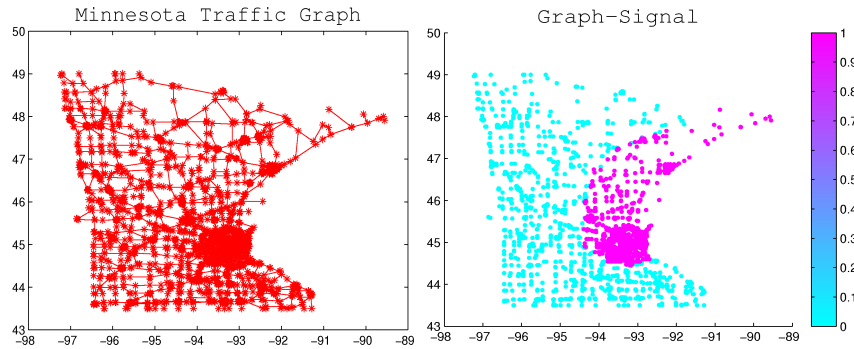


Fig. 9: (a) The Minnesota traffic graph and (b) the scatter-plot of a graph-signal to be analyzed. The colors of the nodes represent the sample values.

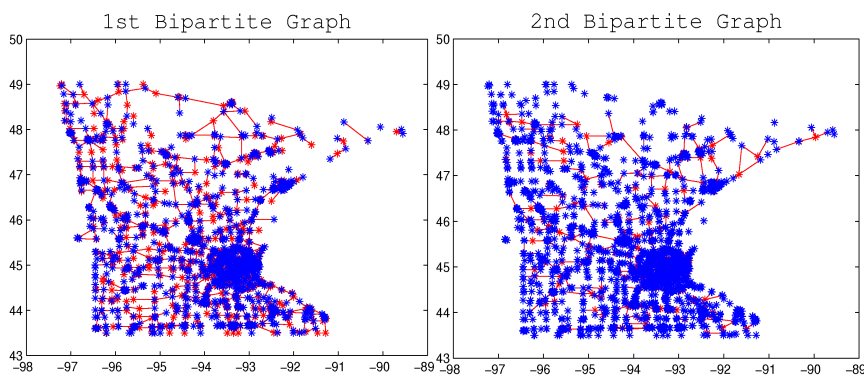


Fig. 10: Bipartite decomposition of Minnesota graph into two bipartite subgraphs using Harary's decomposition.

to perfectly reconstruction, original graph signal from its smooth approximation. In order to see how much energy of the original signal is captured in each channel, we upsample then filter the coefficient of each channel by the synthesis part of proposed filterbank. Figure 12 shows the output of each of the four channel after upsampling/filtering. We see in these plots, that Figure 12(b) is an approximation of the original signal, while Figure 12(c), and Figure 12(d) are the details required to reconstruct the original signal from the approximation.

## V. CONCLUSION AND FUTURE WORK

We have proposed the construction of critically sampled wavelet filterbanks for analyzing graph-signals defined on any arbitrary finite weighted graph. For this we have formulated a bipartite subgraph decomposition problem which produces an edge-disjoint collection of bipartite subgraphs. For these bipartite graphs we have described and proved a *spectrum folding* phenomenon which occurs in downsampling then upsampling ( $DU$ ) operations and produces *aliasing* in the graph signals. Based on this result, we

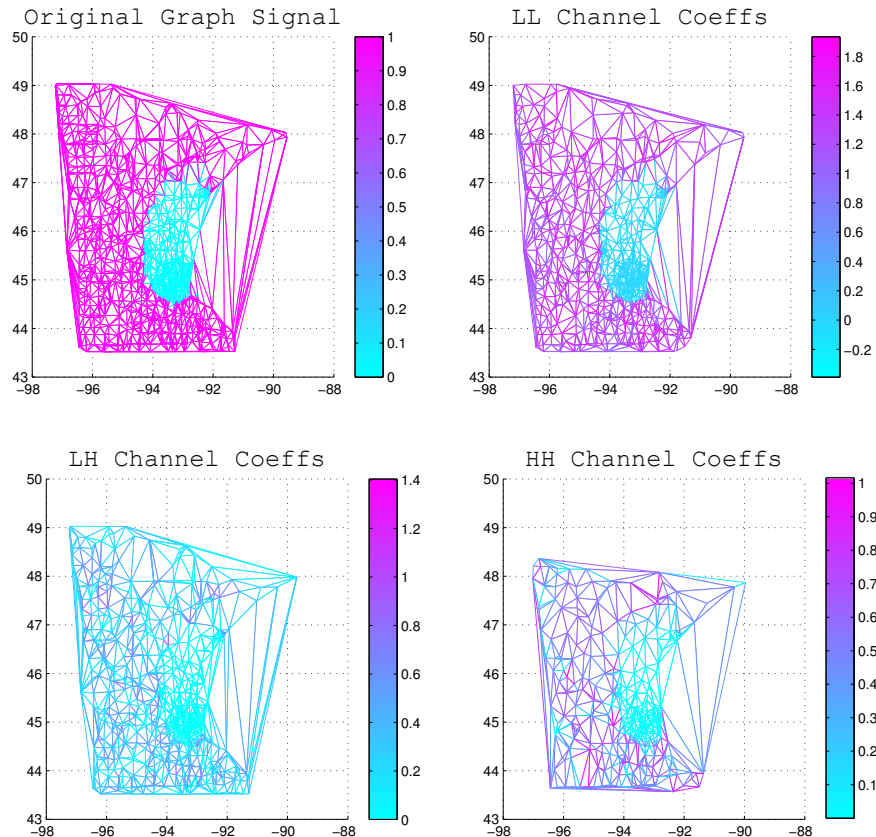


Fig. 11: The Delaunay triangulation plots of output wavelet coefficients of the proposed filterbanks with parameter  $m = 6$ . The edge-color reflects the value of the coefficients at that point. (a) original graph signal (b) LL channel wavelet coefficients (c) LH channel wavelet coefficients (d) HH channel wavelet coefficients

have proposed two-channel wavelet filterbanks on bipartite graphs and provided necessary and sufficient conditions for aliasing cancellation, perfect reconstruction and orthogonality in these filterbanks. As a practical solution, we have proposed a graph-QMF design for bipartite graphs which has all the above mentioned features. The filterbanks are however, realized by Chebychev polynomial approximations at the cost of small reconstruction error and loss of orthogonality. Our current efforts are focused on finding solutions other than the proposed graph-QMF design and to understand and differentiate ‘good’ and ‘bad’ decompositions of arbitrary graphs into bipartite subgraphs.

## VI. ACKNOWLEDGEMENTS

The authors would like to thank Dr. David Shuman at EPFL, for his comments on the first version of the manuscript. We would also like to thank the anonymous reviewers and the associate editor, for their valuable comments and suggestions to improve the quality of the paper.

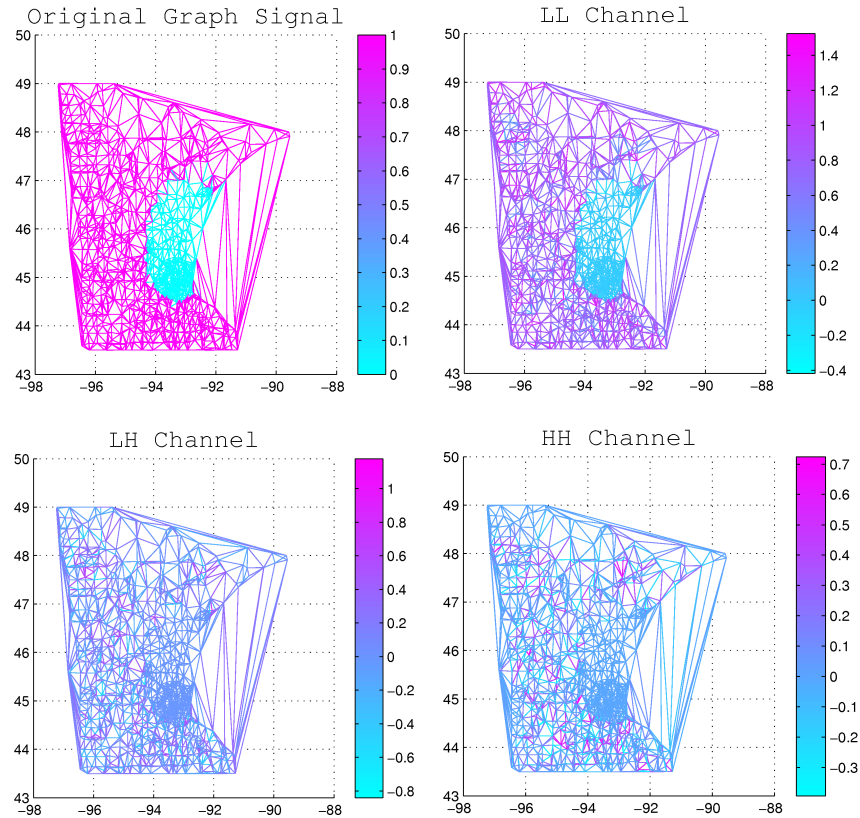


Fig. 12: The Delaunay triangulation plots of the reconstructed graph-signals using the coefficients of a single channel. As before the edge-color reflects the value of the coefficients at that point. (a) original graph-signal (b) reconstruction with LL channel coefficients only (c) reconstruction with LH channel coefficients only (d) reconstruction with HH channel coefficients only

## REFERENCES

- [1] M. Weber and S. Kube, “Robust perron cluster analysis for various applications in computational life science,” in *CompLife*, 2005, pp. 57–66.
- [2] M. Crovella and E. Kolaczyk, “Graph wavelets for spatial traffic analysis,” in *INFOCOM 2003*, Mar 2003, vol. 3, pp. 1848–1857.
- [3] M. Girvan and M. E. Newman, “Community structure in social and biological networks.,” *Proc Natl Acad Sci U S A*, vol. 99, no. 12, pp. 7821–7826, June 2002.
- [4] G. Shen and A. Ortega, “Optimized distributed 2D transforms for irregularly sampled sensor network grids using wavelet lifting,” in *ICASSP’08*, April 2008, pp. 2513–2516.
- [5] W. Wang and K. Ramchandran, “Random multiresolution representations for arbitrary sensor network graphs,” in *ICASSP*, May 2006, vol. 4, pp. IV–IV.
- [6] M. Vetterli and J. Kovačević, *Wavelets and subband coding*, Prentice-Hall, Inc., NJ, USA, 1995.
- [7] R. Coifman and M. Maggioni, “Diffusion wavelets,” *Applied and Computational Harmonic Analysis*, vol. 21, pp. 53–94, 2006.

- [8] David K. Hammond, Pierre Vandergheynst, and Rémi Gribonval, “Wavelets on graphs via spectral graph theory,” *Applied and Computational Harmonic Analysis*, vol. 30, no. 2, pp. 129–150, Mar. 2011.
- [9] R. Wagner, R. Baraniuk, S. Du, D.B. Johnson, and A. Cohen, “An architecture for distributed wavelet analysis and processing in sensor networks,” in *IPSN '06*, April 2006.
- [10] M. Jansen, G. P. Nason, and B. W. Silverman, “Multiscale methods for data on graphs and irregular multidimensional situations,” *Journal of the Royal Statistical Society*, vol. 71, no. 1, pp. 97125, 2009.
- [11] G. Shen and A. Ortega, “Transform-based distributed data gathering,” *Signal Processing, IEEE Transactions on*, vol. 58, no. 7, pp. 3802–3815, July 2010.
- [12] S. K. Narang and A. Ortega, “Lifting based wavelet transforms on graphs,” (*APSIPA ASC' 09*), Oct. 2009.
- [13] S.K. Narang and A. Ortega, “Downsampling graphs using spectral theory,” in *ICASSP '11.*, May 2011.
- [14] Fan R. K. Chung, *Spectral Graph Theory (CBMS Regional Conf. Series in Math., No. 92)*, American Mathematical Society, February 1997.
- [15] U. Luxburg, “A tutorial on spectral clustering,” *Statistics and Computing*, vol. 17, no. 4, pp. 395–416, 2007.
- [16] E. B. Davies, G. M. L. Gladwell, J. Leydold, and P. F. Stadler, “Discrete nodal domain theorems,” *Linear Algebra and its Applications*, vol. 336, no. 1-3, pp. 51 – 60, 2001.
- [17] F. R. K. Chung, *Spectral Graph Theory*, American Mathematical Society, 1997.
- [18] S. K. Narang and A. Ortega, “Local two-channel critically-sampled filter-banks on graphs,” *ICIP*, pp. 333–336, Sep. 2010.
- [19] F. Harary, D. Hsu, and Z. Miller, “The biparticity of a graph,” *Journal of Graph Theory*, vol. 1, no. 2, pp. 131–133, 1977.
- [20] W. Klotz, “Graph coloring algorithms,” *Mathematik-Bericht*, vol. 5, pp. 1 – 9, 2002.
- [21] G. Shen, W.S. Kim, S.K. Narang, A. Ortega, J. Lee, and H.C. Wey, “Edge-adaptive transforms for efficient depth map coding,” in *Picture Coding Symposium (PCS), 2010*, Dec 2010.
- [22] E. Martínez-Enríquez, F. Díaz de María, and A. Ortega, “Video encoder based on lifting transforms on graphs,” .
- [23] D. Scharstein and R. Szeliski, “A taxonomy and evaluation of dense two-frame stereo correspondence algorithms,” *Int. J. Comput. Vision*, vol. 47, pp. 7–42, April 2002.